Dissertation

15d-PGJ_2 – a plausible therapeutic agent against osteosarcoma

Submitted by:

Mateja MIKULČIĆ, MSc

for the Academic Degree of

Doctor of Philosophy (PhD)

at the

Medical University of Graz

Department of Pulmonology

under the Supervision of

Andelko HRZENJAK, Assoc. Prof. PD. PhD.

2022

I hereby declare that this thesis is my own original work and that I have fully acknowledged by name all of the individuals and organizations that have contributed to the research for this thesis. The credit for all the materials used has been made duly acknowledged within the text. Throughout this thesis and in all related publications I followed the *"Guidelines of the Medical University of Graz on Good Scientific Practice".*

Date: 23.07.2022

DISCLOSURES

This dissertation project resulted in the publication of the following scientific paper:

1. Mikulčić M, Tabrizi-Wizsy NG, Bernhart EM, Asslaber M, Trummer C, Windischhofer W, et al. 15d-PGJ_2 Promotes ROS-Dependent Activation of MAPK-Induced Early Apoptosis in Osteosarcoma Cell In Vitro and in an Ex Ovo CAM Assay. Int J Mol Sci. 2021 Oct;22(21).

The data contained in the publication will also be discussed and presented in this thesis.

All of the aforementioned co-authors have explicitly agreed to the use of their data in this thesis.

ACKNOWLEDGEMENTS

This dissertation has been made as a part of the Molecular Medicine PhD program at the Medical University of Graz, with the financial support of the Austrian National Bank. I would hereby like to express my gratitude towards both, as well as towards my supervisor., prof. dr. Andelko Hrzenjak, for his continuous patience, help and support, towards the members of my Thesis Committee, prof. dr. Wolfgang Sattler and prof. dr. Ernst Malle, for their continuous help and advice, to Julia Slanovc, Sandra Kickmaier and Jeannine Budinsky for their assistance in the laboratory, as well as to all of the co-authors and colleagues that took part in helping complete this dissertation project through the past three years.

TABLE OF CONTENTS

I. ABBREVIATIONS AND DEFINITIONS

OS	Osteosarcoma
Rb	Retinoblastoma
MRI	Magnetic resonance imaging
PET	Positron emission tomography
CRP	C reactive protein
PG	Prostaglandin
PGG2	Cyclic endoperoxide prostaglandin G2
PGH2	Prostaglandin H2
COX-1	Cyclooxigenase-1
COX-2	Cyclooxigenase-2
PGD2	Prostaglandin D2
PGE2	Prostaglandin E2
PGF2	Prostaglandin F2
PGDS	Prostaglandin D2 synthase
GPCRG	Protein–coupled receptor
15d-PGJ_2	15-deoxy-Δ12,14-PGJ_2
PPAR-γ	Peroxisome proliferator-activated receptor gamma
MAPK	Mitogen-activated protein kinase
RXRα	Retinoid X receptor alpha
DNA	Deoxyribonucleic acid
SRC-1	Steroid Receptor coactivator-2

AP-1	Activator protein-1
JAK/STAT	Janus kinase/Signal transducer and activator of transcription protein
NF-kB	Nuclear factor-kappa B
TNF-α	Tumor necrosis factor-α
IL	Interleukin
ROS	Reactive oxygen species
CAM	Chorioallantoic membrane
DMSO	Dimethyl sulfoxide
EMEM	Eagle's minimum essential medium
DMEM	Dulbecco's Modified Eagle's Medium
FCS	Fetal calf serum
MTT	3-(4,5-dimethylthiazol-2-yl)-2,5-diphenyltetrazolium bromide
H2DCFDA	5-(and -6)-carboxy-2′,7′-dichlorodihydrofluorescein diacetate
PBS	Phosphate-buffered saline
DCF	Dichlorofluorescein
BCA	Bicinchoninic acid assay
PVDF	Polyvinylidene fluoride
BSA	Bovine serum albumine
TBST	Tris-buffered saline with Tween 20
HRP	Horseradish peroxidase
RT	Room temperature
PFA	Paraformaldehyde
SD	Standard deviation

ERK1/2	Extracellular signal-regulated kinase
NAC	N-acetyl-cystein
PDTC	Pyrrolidine dithiocarbamate
SOD	Superoxide dismutase
PARP	Poly(ADP-ribose)-polymerase
JNK	c-Jun N-terminal kinase
AKT	Protein kinase-B
Nrf2	Nuclear factor E2-related factor 2
Egr1	Early growth response factor 1
NF-κB	Nuclear factor NF-kappa B
Trx	Thioredoxin
ASK1	Apoptosis signaling kinase 1
Trx	Thioredoxin
NADPH	Nicotinamide adenine dinucleotide phosphate
NOS	Nitric oxide synthesase

II. LIST OF FIGURES

III. **ABSTRACT** (English)

Osteosarcoma (OS) is the most often occurring type of bone cancer. It mainly affects children and adolescents and still has a very limited choice of therapy. 15-Deoxy-Δ12,14-prostaglandin J2 (15d-PGJ_2) is a cyclic prostaglandin originating from the arachidonic acid. It is naturally present in the human body and has been known for its remarkable anti-inflammatory as well as anti-cancer effects. In this study, we have investigated the effect of 15d-PGJ_2 on OS cells and the molecular mechanisms that underlie these effects. The cell lines used were of a human origin and osteoblast-like characteristics (U2-OS and Saos-2). The effect of 15d-PGJ_2 on the OS cell lines was explored through observing the effect of the compound on cell survival, cell proliferation, cell motility and tumorigenic capability of the cells, showing a marked decrease of all of the aforementioned tumor cell characteristics. H2DCFDA was used to determine the effects of 15d-PGJ_2 on the intracellular ROS levels, which in turn showed a significant time dependent increase in ROS production. Protein expression analyses via immunoblotting revealed a 15d-PGJ_2-triggered time-dependent increase in MAPK activation (pp38, pJNK and pERK1/2), though the cytoprotective proteins showed mainly a steady decline in their expression. In parallel, immunoblotting and Annexin V/PI staining revealed the presence of strong apoptotic events within both OS cell lines post-15d-PGJ_2 treatment. The *ex ovo* CAM model was used to study the effect of 15d-PGJ_2 on the OS cells growth capability, showing a pronounced impact on the onplant size compared with the control cells. These findings were also confirmed by hematoxylin/eosin as well as Ki-67 immunohistochemical stainings. Lastly, we investigated whether a 15d-PGJ_2 structural analogue, 9,10-dihydro-15d-PGJ_2, could mimic the cytotoxic impact that the original compound had on the OS cells. Our findings suggest that the structural difference between the two compounds, namely a double bond at the C9 atom which is missing in the analogue but is present in our compound of interest, proved to be relevant as the analogue failed to cause any cytotoxic effect in both cell lines. Taken together, our data suggest that 15d-PGJ_2 has the potential of playing a prominent role as an anti-OS natural compound.

IV. **ABSTRAKT** (Deutsch)

Das Osteosarkom (OS) ist die häufigste Art von Knochenkrebs. OS betrifft vor allem Kinder und Jugendliche und hat noch immer eine sehr begrenzte Therapieauswahl. 15-Deoxy-Δ12,14-Prostaglandin J2 (15d-PGJ_2) ist ein cyclisches Prostaglandin, das aus der Arachidonsäure stammt. Es ist im menschlichen Körper vorhanden und ist für seine entzündungshemmende sowie krebshemmende Wirkung bekannt. In dieser Studie haben wir die Wirkung von 15d-PGJ2 auf OS-Zellen, sowie die zugrunde liegenden molekularen Mechanismen untersucht. Die verwendeten Zelllinien waren menschlichen-Ursprungs und hatten Osteoblasten-ähnliche Eigenschaften (U2-OS und Saos-2). Die Wirkung von 15d-PGJ_2 auf die OS-Zelllinien wurde untersucht, hauptsächlich bezogen auf das Zellüberleben, die Zellproliferation, die Zellmotilität und die tumorerzeugende Fähigkeit der Zellen. Eine deutliche Abnahme aller erwähnten Tumorzelleigenschaften konnte gezeigt werden. H2DCFDA wurde verwendet, um die Wirkungen von 15d-PGJ_2 auf die intrazelluläre ROS-Produktion zu bestimmen. Ein signifikanter zeitabhängiger Anstieg der ROS-Produktion wurde gezeigt. Proteinexpressionsanalysen mittels Immunobloting haben eine 15d-PGJ_2-getriggerte, zeitabhängige Zunahme der MAPK-Aktivierung (pp38, pJNK und pERK1/2) gezeigt. Die Expression zytoprotektiver Proteine zeigte eine stätige Abnahme. Parallel dazu zeigten Immunoblotting und Annexin V/PI-Färbung das Vorhandensein starker apoptotischer Ereignisse in beiden OS-Zelllinien nach der 15d-PGJ2-Behandlung. Das *ex ovo* CAM-Modell wurde verwendet, um die Wirkung von 15d-PGJ2 auf die Wachstumsfähigkeit von OS-Zellen zu untersuchen. Dabei konnte ein deutlich vermindertes Tumorwachstum von 15-PGJ2-behandelten Zellen im Vergleich zu Kontrollzellen beobachtet werden. Diese Ergebnisse wurden dann auch durch Hämatoxylin/Eosin sowie immunhistochemische Ki-67-Färbungen bestätigt. Schließlich untersuchten wir, ob ein 15d-PGJ_2-Strukturanalogon, 9,10-Dihydro-15d-PGJ_2, die zytotoxische Wirkung des 15d-PGJ_2 nachahmen kann. Unsere Ergebnisse legen nahe, das eine Doppelbindung am C9-Atom in der 15d-PGJ2 Struktur relevant ist, da das Analogon ohne diese Doppelbindung keine zytotoxische Wirkung erzielte. Zusammengenommen legen unsere Daten nahe, dass 15d-PGJ_2 eine herausragende, natürliche Substanz in Bekämpfung der OS ist.

1. INTRODUCTION

1.1. Osteosarcoma (OS)

1.1.1. General characteristics and epidemiology

Osteosarcoma (OS) is a primary malignant bone tumor [1]. It has a characteristic mesenchymal origin, as all sarcoma-based tumors [2], and is known as the most common type of bone cancer [1, 3]. Although it is quite rare, with an estimated annual incidence of approximately five patients per million persons per year, it nevertheless represents the most common primary malignancy of bone. It presents itself through a dual highest incidence peak, occurring mostly in young adolescents and elderly above the age of 60, although, it shows a highest incidence of occurrence in the ages of early adolescence. It is also the most frequent malignant bone tumor found in children and adolescents in general, preceded only by brain tumors and lymphomas. Annually, on average, osteosarcoma displays an incidence of 5.6 cases per million children under the age of 15 [1, 2-5].

It is important to mention that there has been a commonly made hypothesis regarding the connection between rapid bone growth in adolescence and the increased risk of OS development. This is mainly supported by the tumor's typical metaphyseal location (portion of the bone located at both ends of all long bones – it contains the growth plate which ossifies and increases in size as the person reaches adulthood), its specific highest incidence interval being that between adolescence and early adulthood, as well as by the fact that statistics show how the illness most commonly occurs in active male adolescents (60%). [6-8] The most common areas of the bone where OS is developed are femur (50%), tibia 19.6%, humerus 15.2% and distal fibula 2.2% [9].

Unfortunately, a striking number of patients is discovered to already bear metastases at the time of diagnosis (15-20%), with the metastases mostly occurring in lungs (80-90%) [10]. Less commonly occurring, though more dangerous, is a type of OS metastasis that has spread to other bones and connective tissue. The 5-year survival rate of OS patients who experience this type of metastatic cancer progression is only 13% [2].

All types of metastases present a significant challenge in regards to treatment success and influences the mortality rate of OS patients [2,6]. Namely, only an average of 20-30% of OS patients with any type of metastases present at the time of diagnosis have a chance for a 5-year survival [6, 11-12]. Distinctively, the number of patients with a localized variant of OS which end up developing a cancer recurrence (either local or distal) is a fairly large percentage of approximately 30-50%. Of these relapses, 90% are lung metastases and they are known to

occur within approximately the initial 2 to 3 years following the first appearance of the original OS illness [6,13].

Historically, general 5-year survival rates of all OS diagnosis patients used to be as low as <20% in high-grade conventional osteosarcoma at a time before chemotherapy used to be administered as one of the possible treatment methods. Nowadays, as previously mentioned, the 5-year survival rate of patients with a metastasised form of distal OS is 20-30%, while those suffering from regional or localised OS, when diagnosed sufficiently early and prior to the cancer's spread further from the initial affected area, is 66% and 74%, respectively [2, 15].

A particularly good indicator of either a more favourable or a less favourable survival outcome is the response of the individual's cancer lesions to the administered adjuvant chemotherapy medication. Adjuvant chemotherapy is a common OS therapeutic approach in modern medicine, as it is often administered not only in more wide-spread cases of OS but also both before and after surgical removals of tumour-ridden lesions or body areas, in other to ensure a more certain systemic eradication of any possible presence of cancer in the patient's body, as much as it is individually possible. As will be further mentioned, when OS is diagnosed, up to nearly a quarter of patients (15% up to a staggering 20% of patients, to be more precise) suffer from already present macroscopic signs of metastases (most commonly – in 90% of the cases – within the lungs, 8-10% in the bones and in a very minor amount of cases in the lymph nodes as well) [6, 13, 15].

1.1.2. OS - genetic background

In 70% of the cases, chromosomal aberrations play an important role in the development of OS [5]. OS is known to also often occur in patients suffering from Paget's disease and patients that were previously exposed to radiation therapy. The most common genetic alterations connected to OS development are those of the p53 and retinoblastoma (Rb) genes [4-5]. Strikingly, in the case of patients who suffer from hereditary retinoblastoma, the incidence of OS development is 12.1%. Another example of a potential genetic trigger for this type of cancer is WRN (RECQL-3) gene. Patients suffering from a mutation in this gene (Werner syndrome) show accelerated aging, which usually starts during adolescence and display a 7.7% incidence of OS [2-3, 16]. Mutations in the formerly mentioned p53 gene, commonly occurring in those suffering from the Li-Fraumeni syndrome, are responsible for an increased incidence of OS development in 3% of the patients [16-17]. Viewed from an even

more detailed perspective, it has been shown that there is a total of 14 genes whose mutations are responsible for the occurrence of 87% of OS cases, the genes being: *TP53*, *RB1*, *BRCA2*, *BAP1*, *NUMA1, RET*, *ATM*, *PTEN*, *WRN*, *MUTYH*, *RECQL4*, *FANCA*, *MDC1* and *ATRX* [18].

Generally, the mutational spectrum of OS bears a large likeness to the ageing signature of a high number of so far genetically analyzed malignant tumors. Although, more in-depth analysis has showed that the mutation algorithm bears most similarity to tumors with signature types 3 (breast, ovarian and pancreatic cancer) and 5 (found to be present in all cancer types) [18]. In regards to germline mutations in particular, due to the fact that patients suffering from Li–Fraumeni, Bloom and Werner Rothmund–Thomson syndromes all have an increased risk of OS development [1-3, 18], it is justified that some of the germline mutations found in various types of OS coincide with mutations present in patients suffering from the aforementioned syndromes. These are, namely: a WRN germline mutation (found in OS-230), two TP53 mutations (OS-228, OS-241), as well as two highly rare germline mutations of the RECQL4 gene (OS-227 and OS-238) [18].

In regards to somatic copy-number alterations, they are known to be the mutation types that can affect OS genomes in a greatly varying amount: from making up 0.2% of an OS tumor genotype (as is the case in OS-251) to making even up to 87% of a tumor genotype (OS-038). The most frequent mutation involves changes to the chromosome 8 (changes to this particular chromosome appear in 75% of the somatic copy-number alteration mutations) [17, 18].

1.1.3. Histological classification of OS and diagnosis

The most general classification of OS is that of primary and secondary OS. Secondary OS mainly refers to Paget's OS and radiation-induced OS. [19-20] Primary OS, however, has a more complex subtype division. Primary OS is, therefore, categorized according to the specific anatomical area of the bone where the tumor originates from. Therefore, this this tumor type division includes the intramedullary or central OS, as well a variety of surface OS types. However, the grading also goes into further detail for each of these groups, with the subsequent inner divisions being based mainly on the type of cells involved and affected as well as the aggressiveness of the tumor type.

Needless to say, tumor grading is a crucial step in oncological medicine, as it helps in administering the best and most specific choice of treatment, necessary for the highest possible recovery and survival rate of the patient. A detailed histological categorisation of OS tumors, as declared by the World Health Organisation, is as follows:

- *Central: high-grade, conventional, telangiectatic, small cell, epitheloid, osteoblastomalike, chondroblastoma-like, fibrohistiocystic, giant cell;*
- *Low-grade: low-grade central, fibrous dysplasia-like, desmoplastic fibroma-like;*
- *Surface: low-grade parosteal, intermediate-grade periosteal, high-grade dedifferentiated parosteal, high-grade surface;*
- *Intracortical;*
- *Gnathic (which appears in maxilla and mandible bone);*
- *Extraskeletal: high-grade, low-grade;*
- *Telangiectatic osteosarcoma;*
- *Giant cell-richosteosarcomas (which contain osteoclast-like giant cells);*
- *Small cell osteosarcoma (which is a highly rare histological combination of osteosarcoma and Ewing sarcoma);*
- *Epithelioid osteosarcoma;*
- *Osteoblastoma-like and chondroblastoma-like osteosarcoma.*

The differentiation mentioned above has been established according to several criteria, namely anatomic location, predominant pattern of matrix and histological grade [21].

In further detail, another commonly used grade of tumour is the tumor grading from grade 1 to 4. The percentage of anaplasia and atypia of the cell cytology and histology serves as the most crucial factor in the defining of this type of clinical tumor grading [9, 21].

To further describe the characteristics of low-grade central OS, it is important to mention several facts, among which is that they are known to be very rare and that, histologically, they resemble the low-grade parosteal sarcoma, fibrous dysplasia and other benign lesions. Parosteal osteosarcoma is the most common form of surface osteosarcomas, though, because its diagnosis can be histologically difficult, it is frequently confused with osteoma and osteochondroma. Parosteal osteosarcoma makes up < 0.5% of all diagnosed osteosarcomas and, localisation-wise, 70-83% out of them are located on distal posterior femur [9, 22-23].

High-grade surface osteosarcoma is characterised as such due to its high-grade microscopic characteristics. It is possible to have a high-grade surface osteosarcoma that is a dedifferentiated parosteal osteosarcoma (where the high-grade histological component has replaced the low-grade component). [24] Intracortical OS is another unique type of high-grade OS and, from a histological point of view, it is thought that it is of an osteoid origin. [25] Multifocal osteosarcoma, although very rare, is another major type of high-grade OS and is also its most aggressive form with five year survival being mainly 0% [9, 23, 26].

Accurate diagnostic and staging of OS mainly includes non-invasive radiology procedures such as X-ray imaging of the suspected bone, as well as the adjacent joint. A more in-depth observation of the tumor lesion progression into soft tissue or neurovasculature and surrounding joint tissue is done via magnetic resonance imaging (MRI) and positron emission tomography (PET) [27-28]. The same imaging methods are used to observe and diagnose any present metastases. However, a crucial part of the diagnostic process is the bone biopsy, preferably core biopsy due to a lesser chance of local contamination [29]. Lastly, it is notable to mention that even though tumor growth mildly affects the patient's blood-work results (i.e., an existing possibility of monitoring the level of alkaline phosphatase to assess osteoblastic activity as well as observing higher C-reactive protein (CRP) levels as an indicator of a poorer disease outcome) there are no biochemical laboratory tests specific enough to be used as a proper diagnostic tools for OS classification [1, 30].

1.1.4. Osteosarcoma treatment

At present, surgical treatment remains an often necessary method of tumor removal in cases of OS treatment [1-3, 30]. In regards to the types of surgeries done to treat OS using this method, we can list the limb-salvaging and amputational type of surgery, where the former is done mostly in localised, earlier stages of OS growth and the affected bone, or in most cases limb, can be spared, while the latter requires a full removal of the affected bone and tissue, or limb. [4, 5] While this does provide a very certain removal of specific types of OS lesions before they are able to progress further into the body of the patient, it is still a very severe approach to be utilised, especially when full amputational surgery is required, due to the fact that, as formerly stated, most of the patients requiring such drastic treatment are children and young adolescents [1, 4, 5].

It is also important to note that there are other therapies available, and often necessary, in cases where the OS tumors have progressed deeper and reached the metastatic stage. These are usually radiation and chemotherapy. However, these therapy approaches do not come without potentially heavy risks of their own, as they have been shown to often cause significant and strong long-lasting side-effects in the aforementioned most common age-group of OS patients: children and adolescents. Radiation and chemotherapy treatments at the ages where the body is still undergoing rapid growth and metabolic changes provides a higher risk for permanent harmful imprints of these types of therapy methods not only on tumor cells, as is desired, but unfortunately on healthy cells as well (of both the surrounding tissues, as well as systemically). These can be diagnosed weeks, or in some cases even years post-treatment. Also, even though children can tolerate chemotherapy somewhat better than adults and elderly, it is crucial to state that, in terms of some of the more drastic side-effects, tumorigenic illnesses in children are also known to often progress more rapidly and aggressively than in the older age-groups. Hence, finding an appropriate quick-acting but safe enough of a therapeutic agent or method that won't cause significant long-term issues in these patients can often be a challenge and their discovery and development is a high necessity for OS patients [31-33].

Some of the aforementioned long-lasting side-effects that a child can obtain post-enduring of radiation or chemotherapy as a treatment of OS can include:

- *hormonal imbalance lasting into adulthood (most commonly hormones of the thyroid gland, as well as hormones involved in the reproductive system)*
- *long-term heart issues due to cardiotoxicity (especially a large problem in the case of doxorubicin, a common OS chemotherapeutic) that include damaged heart valves, coronary artery disease, congestive heart failure, carotid artery disease;*
- *haematological issues (increased level of blood clotting);*
- *central nervous system issues (chronic headaches, seizures, loss of the myelin sheath that covers nerve fibers in the brain, nerve damage in the hands or feet, hydrocephalus, cavernomas (clusters of abnormal blood vessels);*
- *bone and joint issues (juvenile osteoporosis, osteochondroma, bone growth arrest, osteonecrosis, chronic pain)* [32-35].

In regards to various types of surgical procedures of tumor removal, amputation holds a slightly smaller rate of tumor recurrence versus removal via limb salvage methods. However, there have been many promising and improving advances in the efficiency and survival rate effects of both resection and reconstruction steps of limb salvage surgical techniques [1,30,40].

When possible, a combination of surgery with a chemotherapy is needed as the most efficient method of OS treatment with the highest survival rate outcome. Introduced as a part of the OS treatment regime in the 1970's, chemotherapy became a staple pre- and post-operative treatment (neoadjuvant and adjuvant treatment, respectively) for OS patients, with the most common chemotherapeutics used being doxorubicin and metothrexamate [1, 14 36-37]. In the recent years, chemotherapeutics with a more molecular classification-based approach have started to be tested and introduced in OS treatment, such as pazopanib and dasatinib with somewhat positive results, but still a relatively high level of toxicity, side-affects and inconclusiveness about its applicability of use for a regular OS treatment [38-41].

Because of the aforementioned facts, it can be concluded that finding an affective, more appropriate and safe method for osteosarcoma treatment is a large priority in the current bone tumor research.

1.2. Cyclopentenone prostaglandins

1.2.1. General introduction and biological properties of prostaglandins

Prostaglandins (PGs) are pivotal bioactive molecules involved in numerous physiological functions. In the past two decades, their strong anti-inflammatory activity has been the biggest focus of PG scientific research [42-43], however, their pronounced effect on the biology of various types of cancers has emerged as an increasingly interesting topic [44-45]. PGs are generated by the cyclooxygenase pathway, originating as arachidonic acid metabolites. Additionally, inflammation processes often involve an inhibition of cyclooxygenase as well as general antioxidant activity. An attenuation of both is commonly shown to assist in the increase of cancer risk as well as in the increase of cancer progression [46]. This connection between the propensity of cyclooxygenase and antioxidant activity suppression to act in a tumor-favorable manner, as well of the prostaglandins' capability enact

effects of a completely opposite nature, is often shown as one of the key reasons why prostaglandins show such a promising anti-tumor potential, which presented itself as a potent and favorable additional group of properties that many prostaglandin compounds carry along with their anti-inflammatory capabilities [44-45, 47-48].

In relation to their importance in bone biology and metabolism, it is important to note that prostaglandins have been known to also hold a prominent role in bone resorption, while also carrying a large role in the general process of bone formation as well. Moreover, they are known to be produced in both: cells responsible for bone resorption, such as osteoclasts, and formation, such as osteoblasts. PGE2, in particular, is known to play a huge role in bone metabolism. It is synthesized in bone cells in a COX-2-dependent manner, however, its bone resorption and creation properties have only been more extensively proven via experimentation with an exogenous application of PGE2. To further elaborate, PGE2 has been shown to influence osteoblastic cells in an RANKL-inducing manner, causing the ligand to bind to its receptors on bone marrow macrophages, resulting in a further differentiation of osteoclast cells. On the other hand, systemic applications and infusions of PGE2 in rats and humans showed that the prostaglandin was also capable, in proper conditions where osteogenic factors were present (such as the transforming growth factor β and basic fibroblast growth factor) that a strong bone mass increase and thus increased bone formation could be accomplished. However, how exactly PGE2 fully effects the bone metabolism when created and set to action *endogenously* is still being elucidated and discussed [49-51].

1.2.2. Classification and biosynthesis of prostaglandins

Prostaglandins are acidic lipids. Originating from arachidonic acid (a type of a polyunsaturated omega-6 fatty acid that serves as a common prostaglandin precursor present in human brain, muscles and liver) they can be synthesized in a variety of mammalian cells. The main triggers for the creation of prostaglandins are usually an array of immunological, chemical or even mechanical stimuli. One of further important characteristics of arachidonic acid is that membrane phospholipids are its most abundant storage points, where most of this fatty acid resides dormant within living cells until it is required for prostaglandin or leukotriene synthesis [52].

In the starting stages of prostaglandin synthesis in particular, an enzyme, phospholipase A2 (and less commonly phospholypase C and diacylglycerol lipase in some cells), is responsible for the initial crucial step required for the synthesis to commence – which is the release of the arachidonic acid. The activation of phospholipase A2 is enabled by increased calcium levels and subsequent phosphorylation of the enzyme. An activated form of the phospholipase A2 that is located in cell cytoplasm is translocated into intracellular membranes, where it comes into contact with the arachidonic acid contained in the phospholipid substrates of membranes. These reactions ensure that the free from of the arachidonic acid can be transformed into cyclic endoperoxide prostaglandin G2 (PGG2), which is than transformed into prostaglandin H2 (PGH2) through the process of peroxidation. Both of these reactions are catalyzed via the activity of bifunctional cyclooxigenase enzymes cyclooxigenase-1 (COX-1) and cyclooxygenase-2 (COX-2). PGH2 is then diffused back into the cell cytoplasm where it has the capability to be converted into prostaglandins D2, E2, and F2alpha (PGD2, PGE2, and PGF2alpha, respectively) with the assistance of cell specific synthases. This synthase activity and the subsequent creation of each of these three prostaglandins depends on the presence of various cell-specific isoenzymes. The type of these isoenzymes varies through different cell types and, therefore, causes the variation in the distribution of each of the three primary prostaglandins across different mammalian cells [52-55].

PGD2, a direct 15d-PGJ_2 predecessor, contributes to cellular migration, apoptosis, and matrix calcification within bone tissue [57]. When describing the synthesis of PGD2 in more detail, it is notable that this specific prostaglandin subtype is produced by two types of prostaglandin D2 synthases (PGDS), one being the lipocalin enzyme (L-PGDS, an enzyme regulated by estradiol and present in the brain) and the hematopoietic enzyme (H-PGDS), mostly present and active in the immune system as well as in mast cells. The main interactions of PGD2 are made through its binding to the G protein–coupled receptors (GPCRs) DP1 and DP2. Already this prostaglandin type has been shown to carry strong potential for anti-inflammatory activity [57-58].

Due to the fact that PGD2 is highly unstable, it is capable of being efficiently converted into the biologically active cyclopentenone J2 prostaglandins through spontaneous dehydration, which is a reaction that is commonly dependent on serum albumin levels. These J2 prostaglandins include PGJ2, Δ12-PGJ2, as well as 15-deoxy-Δ12,14-PGJ_2 (15d-PGJ_2), which is our prostaglandin of choice in this work [58-60].

PGE2 is a further member of the prostaglandin family and is its most abundant member in the mammalian cells. It is synthesized by a variety of solid tumors, acting as a strong modulator of immunosuppression, proliferation, angiogenesis, and invasion of tumor cells [61-62].

Prostaglandin I2, another well-known prostanoid, is known to be synthesized and present mostly in endothelial cells, with the stabilized form of prostacyclin synthase being the key component for the synthesis [44, 63].

During an inflammatory response, both the level and the profile of general prostaglandin production within the human body changes dramatically. The prostaglandin production is usually very low in tissues that are stable and unaffected by stress and inflammatory processes, but it increases very rapidly, serving as a cellular mechanism activated prior to leukocyte activation and the infiltration of immune cells – all of which occur in the state of acute inflammation [58].

While both main cyclooxygenases (COX-1 and COX-2) have an equal potential to facilitate the above mentioned prostaglandin synthesis chain, they both have the possibility to trigger the generation of homeostatic and autoregulatory prostanoids. Both have been proven to assist with the release of prostanoids during inflammatory responses, although they do vary in their particular localizations. COX-1 is known as the dominant source of prostanoids and is expressed in most all cell types. Its activity supports cellular housekeeping functions and homeostasis in a variety of bodily tissues. COX-2, on the other hand, is mainly activated only through unique conditions present after cellular reactions to inflammatory stimuli, growth factors and hormones. It is known to particularly be crucial for prostanoid formation in the state of active inflammation as well as being increased and active in various proliferative and cancerous diseases where it is released in tumor microenvironment to act in a manner supportive to tumor survival and metastasis [42, 64].

The ultimate stable degradation product of the PGD2 metabolism is 15d-PGJ_2 (organic structure shown in **Image 1.**). Many of the effects of 15d-PGJ_2 on various cellular responses are based on the distinct electrophilic character of this lipid. To further elaborate, the stable 15d-PGJ_2 contains a unique cyclopentenone ring structure that is characterized by the presence of a chemically reactive α,β-unsaturated carbonyl group that is hypothesized to potentially play one of the key roles in the many effects that this prostaglandin compound can exert on cells such as immune as well as cancer cells and tissues. This has been showed to mainly occur because the reactive cyclopentenone ring of this prostaglandin often very easily react with any nucleophilic groups-containing substances, offering a wide variety of possible

interactions within a plethora of biological organism cells [65, 91]. Under basal conditions, picomolar to nanomolar concentrations of free 15d-PGJ_2 have been measured in biological fluids. In particular, the levels of 15d-PGJ_2 in samples of healthy human plasma range between 2.5 and 349.6 pg/mL [66].

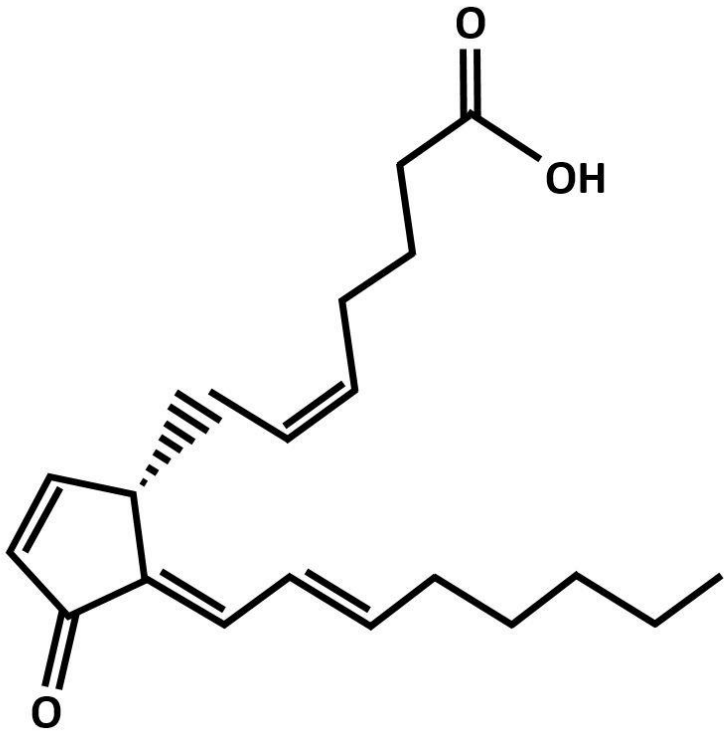

Image 1. ***Organic structure representation of the 15d-PGJ_2 compound***

1.2.3. 15-deoxy-Δ12,14-PGJ_2 – potential clinical relevance

Through time, 15d-PGJ_2 has been shown to be a very promising compound in medical context due to its strong effects in regards of influencing immunological responses [43, 59] and viability of cancerous cells [43, 67]. The mechanisms used to achieve these effects are complex and still not fully elucidated. So far, more is known about its anti-inflammatory and

antioxidant effects on certain immune cells, while its anti-tumorigenic effects show effects of an opposite type and have only been more researched in approximately the last decade.

One of the key factors that seems to be included in the effects of 15d-PGJ_2 on immunology-related cellular mechanisms is PPAR-γ. The N-terminal region of PPAR-γ holds a mitogen-activated protein kinase (MAPK) phosphorylation site. 15d-PGJ_2 interacts with this phosphorylation site in a way that, when 15d-PGJ_2 enters the cell, it binds to the PPAR-γ molecule, resulting in a formation of heterodimers combined with retinoid X receptor alpha (RXR α). Following this, the formation is bound to specific sequences of the cell deoxyribonucleic acid (DNA), thus causing the activation of certain target genes [59, 68]. To better understand the interaction between 15d-PGJ_2 and PPAR-γ, it is important to know that 15d-PGJ_2 contains a carboxylic acid as its polar head. The hydrogen bond interactions, where the lipid molecule docks with the receptor, have been found to be, among others, between the aforementioned acid head and the residues of Tyr473 (13.2 %), His323 (12.1 251 %), Ser289 (13.2 %), His449 (10.5 %), and Gln286 (4.7 %) of the PPAR-gamma ligand [68-69]. The interaction of the lipid molecule and the ligand can also induce a specific interaction of the subsequent PPAR gamma/RXRα combination with up to 369 steroid receptor coactivators-1 (SRC-1) [68]. This ligand activation has also been found to affect the activator protein-1 (AP-1), the Janus kinase/Signal transducer and activator of transcription protein (JAK/STAT) pathway, as well as the nuclear factor-kappa B (NF-kB), which all play prominent roles in cell immunity and inflammatory responses [44, 70]. The impact of 15d-PGJ_2 on all of the aforementioned proteins and protein pathways results in an anti-oxidative suppression of inflammation [43, 59]. This effect is also enabled by PPAR-gamma being expressed, among other locations, in human monocytes. When 15d-PGJ_2 binds to the PPAR-gamma receptor within human monocytes, it shows a clear inhibition of macrophage activity [71-72]. PPAR-gamma is also commonly expressed in endothelial cells where 15d-PGJ_2 can bind to it and cause a similar anti-inflammatory response [71, 73].

An additional inflammation-protective mechanism that 15d-PGJ_2 induces in macrophages in a PPAR-gamma dependent way is through its negative effect on the macrophages via Egr1 decrease [74]. Through similar PPAR-gamma related mechanisms, 15d-PGJ_2 has been shown to successfully reduce allergy-induced pulmonary inflammation via an inhibition of pro-inflammatory cytokines tumor necrosis factor-α (TNF-α) and interleukin(IL)-10 production [75]. Similar mechanisms were also observed in murine models of asthma, where inflammation is suppressed through an inhibition of the TNF-α, IL-5, IL-13 and IL-17 activity through PPAR-gamma dependent targeting of the NF-kappa B signaling pathway [76].

It has also been found that 15d-PGJ_2 has an anti-inflammatory role in the nervous system [77-78], pancreas [79], chondrocytes [80] and in the liver [81]. Additionally, 15d-PGJ_2 has been found to be able to successfully regulate T-cell activation, as well as the expression of inflammatory cytokines by enhancing PPAR-gamma transcriptional activity [59].

In the past decade and a half, investigations on potential anti-cancer effects of 15d-PGJ_2 increased as well, versus the prior bigger emphasis on its effects on various immunological reactions. Thus, a series of studies have been done on this subject.

A ligand that 15d-PGJ_2 commonly uses in order to achieve its anti-cancer properties is the previously mentioned PPAR-gamma [67]. A common mechanism that 15d-PGJ_2 uses to achieve these anti-cancer effects is the increase of reactive oxygen species (ROS) levels, which then upregulates cancer cell apoptosis [82-83]. Some examples of the 15d-PGJ_2 and cancer cell interactions where it can induce such pro-apoptotic behavior is the reaction of 15d-PGJ_2 with non-small lung cancer cell carcinoma, glioma [44, 67], colorectal cancer, leukemia [84], as well as thyroid papillary cancer [85]. Another mechanism by which the 15d-PGJ_2 and PPAR-gamma interaction can cause cancer cell death is via the inhibition of telomerase activity, which in turn, leads to senescence and death of the impacted cells [67, 86].

However, even though 15d-PGJ_2 is an endogenous ligand of the PPAR-gamma and often enacts its effects in dependence of it, it can also cause its damaging effects on cancer cells in PPAR-gamma-independent ways. Some cancer types where this has been observed are lung cancer [87], renal cancer [88] breast cancer [89] and leukemia cells [90].

Altogether, it can be concluded that there have been many studies done which highlight the potential of 15d-PGJ_2 and the assistance as well as an important role that it could play in search for an appropriate combatant against a great variety of tumors. However, it is important to note that a great deal of the deeper mechanisms underlying the prostaglandin compound’s intracellular actions which lead to the aforementioned favorable anti-cancer properties still remain somewhat unexplored.

1.2.3.1. 15-deoxy-Δ12,14-PGJ$_2$ and osteosarcoma

Even though many of the inner metabolic and molecular details and mechanisms triggered by 15d-PGJ$_2$ on OS cells are still unknown and require further research, the general effects of 15d-PGJ$_2$ on OS cells have been previously described to a certain extent, providing a solid and promising basis required to encourage a more extensive type of research on this subject. Notably, our group showed that the simultaneously cytotoxic and cytoprotective effects of 15d-PGJ$_2$ on OS cells are based on the activation of the MAPK/Akt/Nrf2 axis. This study showed the initial promising aspects of the strong effect this lipid compound had on OS, namely MG-63. However, the effects revealed upon this particular cell line portrayed a very dual nature. On one hand, it was shown that 15d-PGJ$_2$ caused a significant reduction in cell metabolic activity and an increase in PARP cleavage. Additionally though, a very strong anti-apoptotic effect was discovered simultaneously, marked with a strong rise in the expression of proteins belonging to the HO-Nrf2 axis [91].

Yen at al. included U2-OS and, to a smaller extent, the Saos-2 cell line as well, and aimed to elucidate the similarly observed antioxidant effects of 15d-PGJ$_2$ on the OS cell lines. Within their results, they portrayed how the lipid substance induces a ROS-mediated Akt inhibition and cell cycle alterations [92].

However, it is important to note several aspects of the results of both of the aforementioned groups. Our previous work, in the paper by Koyani et al., focused only on one cell line (MG-63) [91]. Yen et al. showed the effects of 15d-PGJ$_2$ on three different cell lines (MG-63 U2-OS and Saos-2), but only in regards to long term treatments spanning mostly above 24 hours of exposure to the compound, which leaves us with many unanswered questions about the very beginning and initial triggering of 15d-PGJ$_2$ when displaying its effects on these OS cell lines, as well as the characteristics of the more acute effects of the compound [92].

It is safe to say that many of its molecular mechanisms in different OS cancer cells are still not fully elucidated and what both studies lacked was a more in-depth analysis of other viability effects of the prostaglandin on the OS cells, such as whether it asserts its effects on particular oncogenic properties such as cell motility and multiplication (colony forming ability), as well as an attempt of testing the substance's effect on a model other than cell culture. As we began our most recent study, we aimed to attempt an approach that went in further depth regarding all of the mentioned issues, as well as confirming and strengthening some of the conclusions presented so far via provision of additional data.

Therefore, our work focused on the hypotheses that:

- *15d-PGJ_2 indeed exhibits a strong apoptotic effect on OS cell lines (U2-OS and Saos-2), however, we believed that this is present already at the earliest stages of cell treatment in a manner heavily dependent on the quick activation intracellular stress via increased ROS production, which in term triggers MAPK phosphorylation and consequently cell apoptosis.*
- *The apoptotic effects of 15d-PGJ_2 on OS cells might have a strong effect on, in particular, cell motility and colony forming ability, all within the first 24 hours of treatment.*
- *When applied to a treatment model involving the use of a living membrane (chicken chorioallantoic membrane, CAM), the negative effects of the substance would be seen in the way similar to that in cell culture experiments.*

Following the current available scientific knowledge of these topics, as well as the main points on which we have based the general direction of our hypotheses regarding the intracellular effects that 15d-PGJ_2 may have on the U2-OS as well as Saos-2 cell lines, we then proceeded to focus the aim of our research into this topic by utilizing the following experimental approaches:

1. the exploration of cell viability effects post-15d-PGJ_2 treatment as well as their characteristics;
2. the exploration of the apoptotic effects upon the cells post-15d-PGJ_2 treatment as well as their characteristics (and, if possible, a comparison of the apoptotic effect strength with a cell line serving as a non-cancer equivalent of the OS);
3. the exploration of MAPK behaviour both independently and in regards to ROS post-15d-PGJ_2 treatment;
4. the exploration of any potential anti-oxidant or anti-apoptotic effects upon the cells post-15d-PGJ_2 treatment;
5. the observation of the 15d-PGJ_2 effect on the OS cells when grown on a live CAM model.

Ultimately, through our results we have successfully confirmed that 15d-PGJ_2 has pronounced cytotoxic effects in the two OS cell lines which we focused on, namely, U2-OS and Saos-2, as well as a promisingly smaller effect that this prostaglandin compound has on

a cell line serving as a non-cancer cell equivalent of the OS based on the tissue of origin of OS cells – this being *the bone*, while the cell line in question is *an osteoblast cell line* hFOB 1.19. Additionally, to further describe our conclusions regarding or experimentation on the OS cells, the cytotoxic effects we observed were largely based on the ROS-mediated apoptosis induction. These effects were also stronger in OS cell lines compared to its effects on non-malignant osteoblast cells. Furthermore, we have also proven strong inhibitory effects of 15d-PGJ_2 on OS-tumor growth through the usage of the chick *ex ovo* chorioallantoic-membrane (CAM) assay, this being an important step in *in vivo* direction and future clinical studies. This thesis aims to explain and present all of our conclusions in detail, as well as to reflect on their significance and the future of 15d-PGJ_2 in context of its significance within the field of OS treatment research.

2. MATERIALS AND METHODS

2.1. 15d-PGJ_2 preparation

The main substance used in this study was 15d-PGJ_2 (15-deoxy-$\Delta^{12,14}$-prostaglandin J_2, #18570) – a prostaglandin compound obtained from the Cayman Chemical Company, Ann Arbor, MI, USA. The substance was originally dissolved and shipped in methyl acetate (stored at -20°C), which was removed via the process of desiccation prior to further substance preparation required for the experiment-related cell treatments. In order gain a substance form usable for cell treatments, 15d-PGJ_2 was next dissolved in a vehicle solution – dimethyl sulfoxide (DMSO, Sigma-Aldrich, MO, USA) under sterile conditions. The resulting stock solution was aliquoted (20 mM) and stored at -20°C. The aliquots were then used within two weeks. As mentioned, and unless the individual experiment descriptions state otherwise, DMSO was used as a vehicle control, with its concentration matching the 20 μM concentration of 15d-PGJ_2 (0.04%, v/v) that had been used in the experiments.

2.2. Cell culture procedure

The media and cell culture substances were all obtained from Gibco (Thermo Fisher Scientific, Schwerte, Germany). The cell growth media contained 10% fetal calf serum (FCS) obtained also from Thermo Fisher Scientific and heat-inactivated in our through a 56°C incubation of the medium for 30 min. This was done with an aim to destroy complement activity within the serum which might disrupt a number of observed and measured intracellular as well as intercellular events, causing the measured and observed data within experiments to be unrealiable – heat inactivation greatly reduces the risk of this happening and of the existence of any unwanted complement activity.

All of the used OS cell lines (U2-OS [HTB-06], Saos-2 [HTB-85], MG-63 [CRL-1427]) are of human origin and epithelial (U2-OS and Saos-2) or fibroblast (MG-63) morphology. The U2-OS is known to be derived by J. Ponten and E. Saksela in the second half of the 20th century, with the cell line originating from a moderately differentiated sarcoma of the bone of a 15-year-old, white, female osteosarcoma patient (possible patient therapy unknown). The Saos-2 was derived by J. Fogh and G. Trempe in the second half of the 20th century and originating from the bone of a 11-year-old, white, female osteosarcoma patient treated with methotrexate, adriamycin, vincristine, cytoxan, aramycin-C and radiation therapy. The MG-63

cell line was derived by the Orthopedics Department staff of the University of Leuven hospital in the second half of the 20th century, originating from the bone of a 14-year-old, white, male osteosarcoma patient (possible patient therapy unknown) (ATCC, Manassas, VA, USA). The osteoblast line used (hFOB 1.19) is also of human origin, derived by S. A. Harris and T. C. Spelsberg and established via a transfection of limb tissue obtained from a spontaneous miscarriage with the temperature sensitive expression vector pUCSVtsA58 and the neomycin resistance expression vector pSV2-neo (ATCC). Unlike the osteosarcoma cells, the osteoblast cells were not obtained from ATCC but from the Core Facility of Alternative Biomodels & Preclinical Imaging of the Medical University Graz.

Two of the cancer cell lines used, U2-OS and MG-63 cells, had been cultured in an Eagle's Alpha-Minimal Essential medium (EMEM) supplemented with 10% (v/v) FCS, 2.5 mM (w/v) L-glutamine and 1% (v/v) penicillin/streptomycin (Gibco). The Saos-2 OS cells, however, had been cultured in a McCoy 5A medium (Lonza, Switzerland) supplemented with 10% (v/v) FCS, 2.5 mM (w/v) L-glutamine and 1% (v/v) penicillin/streptomycin. The medium of choice used for the osteoblast cell line was a 1:1 (v/v) mixture of Ham´s F12 medium and Dulbecco´s Modified Eagle´s Medium (DMEM) supplemented with 2.5 mM (w/v) L-glutamine, 10% (v/v) FCS, 1% (v/v) penicillin/streptomycin, and 0.3 mg/ml G-418 (Geneticin, InvivoGen, Toulouse, France). All three cancer cell lines were incubated and cultivated at 5% CO_2, 37°C and 98% humidity, while the hFOB 1.19 cell line was grown at matching CO_2 and humidity conditions, but at a 34°C.

For all cell lines, the medium was exchanged twice per week and the cells were split once per week at a 80-90% confluence. The exact cell number needed for splitting and for individual experiments was measured by CASY (OMNI Life Sciences, Bremen, Germany). The cells underwent mycoplasma testing every three months in order to assure cell health.

2.3. Cell viability and metabolic activity assay (MTT)

In order to assess the viability and metabolic activity status of 15d-PGJ_2-treated U2-OS, Saos-2 and hFOB 1.19 cells, MTT assay was used. 180 000 cells were seeded per well in 12-well plates and incubated for 24 hours. Afterwards, the cells were treated with 20 µM 15d-PGJ_2 (which was the average commonly used concentration previously described in several studies [59, 84-85, 93-95] for 4, 18 and 24 hours. Following this, the cells were

exposed to the MTT dye (3-(4,5-dimethylthiazol-2-yl)-2,5-diphenyltetrazolium bromide) (concentration of 0.5 mg in serum-free medium) for 30 minutes at 37°C. This resulted in a reaction between the MTT compound and the viable cells, where the still living cells with an active cell metabolism were now stained with the insoluble *formazan* (shown with the viable cells obtaining a dark purple hue). The *formazan* was then made soluble by adding 350 µl of acidic isopropanol (0.04 M HCl in pure isopropanol), enabling us to collect and quantify the reactions within each separate sample. This analysis was then done by the optical measurement by using a microtiter plate reader (BMG Labtech, Ortenberg, Germany) in order to obtain numerical values of the observed cell reaction (the emission/correction wavelengths used for the optical measurement were that of 570/630 nm). This numerical output allowed us to compare the values received for each sample with the vehicle control, the results of which were then also confirmed and assessed with statistical analysis of the multiple measurements, as well as the significance of the data. The total number of experiments used for the statistical analysis was 3.

2.4. Wound healing assay (*Scratch* assay)

In order to be able to investigate the effect 15d-PGJ_2 has on cell proliferation and motility, we applied the wound healing assay, also known as the *scratch assay*. The method was done by seeding the cells in silicone inserts (Ibidi GmbH, Graefelfing, Germany) carefully positioned inside 12-well plates. Once seeded, the cells were left to grow until the confluence of approximately 90% before incubation with 20 µM 15d-PGJ_2 or a 0.04% DMSO as a vehicle control for 24 h, while the inserts were still in place and intact. Once the desired confluence was achieved, the silicone inserts were removed, resulting in a 500 µm cell-free gap being left between two areas of confluent cells (medium was changed in order to remove any dead cells and detritus). Photographs were then taken of the 0 hour time-point and the cells were further incubated at standard cell culture conditions before taking additional photos of the cells at the 24, 36, and 48 hour time-points. The light microscope and camera used for this was Nikon ECLIPSE Ts2, with a 40 x magnification.

The resulting condition of the scratch was then measured from the obtained photos via Fiji ImageJ Wound Healing plug-in (open source), giving us data which were further quantified as percentage of the open scratch area. The percentage was used to make comparisons of the condition of the scratch area in the case of treated vs. untreated cells and these values

were then appropriately analyzed through statistics, confirming their significance. The number of individual experiments used for the statistical calculations was 3.

2.5. Colony formation assay

300 000 cells were seeded pro-well in 6-well plates and incubated for 24 hours. After this, the cells were treated with 15d-PGJ_2 (20 μM) or the corresponding vehicle control (0.04% DMSO) for further 24 hours. Afterwards, cells were trypsinized in order to be counted (all cell counting was done via the Casy cell counter), following which 300 U2-OS cells and 1 000 Saos-2 cells were seeded per-well in a 6-well plate (due to the significantly lower cell multiplication time of the Saos-2 cells). Both OS cell lines were then incubated at 37°C until a certain amount of colonies containing at least 50-cell were formed in the control wells (10 days for U2-OS cells and 15 days for Saos-2). The colonies were then fixed in the 6-well plates using the methanol:glacial acetic acid mix (3:1 [v/v]) and stained with a 0.4% aqueous crystal violet solution (C6158, Sigma).

The stained colonies were then scanned against a clear, white background and counted with the help of the ImageJ software (Colony Counter plug-in). The numerical output was further observed through statistical calculation and the confirmation of data significance. The total number of individual experiments used for the analysis was 3.

2.6. Intracellular ROS measurement (ROS assay)

In order to assess the shift in the production of reactive oxygen species (ROS) in the OS cells before and post-15d-PGJ_2 treatment, we performed a ROS assay. Firstly, 80 000 OS cells per well were seeded in 24-well plates and incubated until a confluence of approximately 80% followed by a treatment with 15d-PGJ_2 (20 μM). Cells were then additionally treated with carboxy-H_2DCFDA (5-(and -6)-carboxy-2′,7′-dichlorodihydrofluorescein diacetate, Invitrogen), a ROS-reactive dye in phosphate-buffered saline (PBS), and incubated at 37°C for 30 minutes. Following this incubation, the cells were washed with ice-cold PBS twice and an incubation in 300 μl of 3% (v/v) Triton X-100 in PBS for 30 min was used to induce cell lysis, additionally enhanced by a further incubation in 50 μl absolute ethanol for 15 minutes (with shaking at

1350 rpm) at a temperature of 4°C. Afterwards, the cell lysates were gathered and centrifuged at 10 000 rpm (at 4°C) in order to remove any cell debris that might hinder upcoming fluorometric measurements. The remaining supernatants and the amount of DCF (2´,7´-dichlorofluorescein) they contained was measured by a microtiter plate reader (CLARIOstar, BMG Labtech, Ortenberg, Germany) at emission levels of 485 nm, as well as an additional correction measurements at 540 nm wavelength. The resulting values are calculated based on the data from 3 independent experiments.

2.7. Immunoblot analysis

First, 300 000 cells were seeded in 6-well plates and incubated for 24 hours at 37°C until they reached a confluence of approximately 80%. Then, the cells were treated with either a 0.04% DMSO vehicle control or 20 uM 15d-PGJ_2 for various time intervals. Five, 10, 15, 30 and 60 minutes were the treatment points used for the MAPK testing time kinetic experiment. One, 2, 4, 6 and 8 hours were the treatment points used for the antioxidant protein expression time kinetic experiment. Lastly, 4, 8 and 12 hours were the treatment time-points used to test the expression of pro-apoptosis proteins. The cells were then washed twice with cold PBS and harvested as well as lysed in RIPA buffer (Sigma, R0278) enriched with phosphatase inhibitors (A32957, Thermo Scientific) and protease inhibitor (A32953, Thermo Scientific). Sonication was used to enhance cell lysis (twice, for 5 seconds), followed by centrifugation at 13 000 rpm for 10 min in order to separate soluble total proteins in the samples.

The supernatants were then collected and the resulting total cell protein amount in the supernatants was measured using a BCA protein assay kit (Thermo Fisher Scientific). Using the results obtained from this analysis, we used 15 µg total protein extracts per sample and denatured them for 10 min at 95°C in order to prepare the samples for electrophoresis. Electrophoresis was used to separate the proteins on a polyacrylamide gel. In the next step, the proteins were transferred from the gel onto nitrocellulose or PVDF membranes (0.45 µm, Amersham) (the PVDF membranes were only used for the expression analysis of Pro-caspase 7, specifically). All membranes were blocked with either bovine serum albumin (BSA) or 5% (w/v) non-fat milk for 1 hour at room temperature (approximately 25°C). The membranes were then incubated overnight at 4°C with a primary antibody solution listed in *Table 1*.

ANTIBODY	COMPANY	CATALOGUE NR.	HOST	DILUTION	POLYACRYLAMIDE GEL%
PJNK	Cell Signaling	#4668	rabbit	1:1000	10%
JNK	Cell Signaling	#9252	rabbit	1:2000	10%
PP38	Cell Signaling	#9211	rabbit	1:1000	10%
P38	Cell Signaling	#9212	rabbit	1:2000	10%
P-ERK1/2	Cell Signaling	#9106	mouse	1:1000	10%
ERK1/2	Cell Signaling	#9102	rabbit	1:2000	10%
P-AKT (SER473)	Cell Signaling	#9271	rabbit	1:1000	8%
AKT	Cell Signaling	#9272	rabbit	1:2000	8%
NF-KB (P56)	Cell Signaling	#8242	rabbit	1:1000	8%
EGR1	Cell Signaling	#4154	rabbit	1:1000	8%
NRF2	R&D Systems	#MAB3925	mouse	1:500	8%
PARP	Cell Signaling	#9542	rabbit	1:1000	10%
CL. CASPASE-7	Cell Signaling	#9491	rabbit	1:1000	12%
ALPHA-TUBULIN	Cell Signaling	#2125	rabbit	1:2000	8, 10, 12%

Table 1. *Primary antibodies and dilutions used in immunoblot experiments (reproduced from [96] with permission of MDPI publisher, Basel, Switzerland).*

The following day, the membranes were washed in TBST (three times, for 10 minutes), after which they were incubated with appropriate secondary antibodies linked with horseradish peroxidase (HRP). Ultimately, the membranes were developed and protein signal visualized via the usage of ECL Prime Western Blot Detection Reagents (Amersham) on a Chemi-Doc Touch Biorad device. Between two different primary antibody incubations, membranes were stripped through an 8 minutes incubation in the Restore Plus Western blot stripping buffer (Thermo Fisher Scientific) and re-blocked. For each protein, the loading control used for expression normalization were either the expressions of the total protein variants (in the case of MAPK proteins) or α-tubulin (for all other proteins). Normalization of the signal intensity of our visualized proteins was done by the Image Lab software 6.0.1 (Biorad). The resulting expression intensities were then statistically analyzed and their significance was tested. The total number of individual experiments used for the statistical analysis of each different experiment resulting in the immunoblot analysis was 3.

2.8. Annexin V/propidium iodide (PI) apoptosis staining

180 000 cells were seeded per-well in 12-well plates and left to incubate at 37°C until reaching a confluence of approximately 80%. The OS cells were then treated with 15d-PGJ_2 (20 μM) for 12, 18 and 24 hours. The cells were then incubated and stained with the FITC Annexin V Apoptosis Detection Kit 1 (BD Biosciences), washed in cold PBS, and incubated for 15 minutes at room temperature (approximately 25°C) with 100 μl of 1 x binding buffer (5 μl of Annexin V FITC and 5 μl of PI) while also being protected from light.

The resulting cytometric analysis was obtained via the Guava EasyCyte 8 (Millipore) flow cytometer and analyzed bythe InCyte 3.1 software (Millipore). The obtained numbers were then statistically analyzed and had their significance confirmed with the total number of individual experiments used being 3.

2.9. *Ex ovo* chicken chorioallantoic (CAM) assay

As a method bridging the gap between *in vitro* and *in* vivo, we used the chorioallantoic membrane (CAM) assay. The specific method was an *ex-ovo* CAM method [94]. Fertilized white Lohmann chicken eggs were carefully cleaned and incubated at 37.5°C and 60% humidity (Incubator Easy 200, J.Hemel Brutgeräte, Verl, Germany). On the third day of the embryonic development, the egg shell was cautiously cracked into a sterile weigh boat, followed by an incubation at 37.5°C and 60% humidity for 6 more days.

In parallel, OS cells (U2-OS, Saos-2, and MG-63) were grown until approximately an 80% confluence and treated either with a DMSO vehicle control or 15d-PGJ_2 for 24 hours. On the ninth day of the embryonic development, before the lymphatic system of the embryo begins developing (in order to avoid potential interferences of the lymphatic development with the resulting tumor growth), the collected OS cells were grafted on CAM into silicone rings (Ø 5 mm) which were carefully placed between embryonic blood vessels ($1x10^6$ cells were added per-onplant). The embryos were incubated for 4 more days at 37.5°C after which the onplants were photographed and harvested via excision. The excised onplants were fixed in 4% paraformaldehyde (PFA), as well as dehydrated and embedded in paraffin wax. The resulting paraffin blocks were cut (into 7 μm thick sections) and fixed on glass tissue slides to be used for immunohistochemial staining. The size of the onplants was also measured from the

obtained photographs and analyzed via statistical analysis (5 representative onplants were used for the statistical comparison of each condition, treated and untreated).

2.10. Immunohistochemistry of the CAM slides

The immunohistochemical staining was made for Ki-67, a proliferation marker, and it was performed in the automated system DAKO OMNIS, using the primary DAKO anti Ki-67 antibody Clone MIB-1 (GA62661-2) as well as the DAKO OMNIS Flex HRP detection system. All of the slides were photographed with the Nikon Eclipse E400 microscope and Zwo Asi 183 MC pro camera. The resulting immunohistochemical staining was evaluated by two experienced colleagues (Dr. Martin Asslaber, Dr. Nassim Ghaffari Tabrizi-Wizsy).

2.11. Statistical calculations

The statistical calculations for all of the experimental data were performed by GraphPad Prism (v. 5.0). All of the obtained values are represented as mean ±SD of at least 3 individual experiments. A two-sided student´s t-test was used to determine the level of statistical differences between samples and a $P \leq 0.05$ value was considered as statistically significant.

3. RESULTS

3.1. 15d-PGJ_2 inhibits the cell growth, colony formation, and motility of human OS cells.

In order to assess if there is an effect of 15d-PGJ_2 on osteosarcoma cells viability and how this effect is demonstrated, we preformed several viability assays with U2-OS and Saos-2 cells treated with 15d-PGJ_2. The concentration of 15d-PGJ_2 chosen for the cell treatments was 20 μM, which is an average concentration gathered through observance of multiple types of data published not only in our previous study with MG-63 cells, but also in a variety of other research papers which utilized the treatment of various types of cancer cells with 15d-PGJ_2. [59, 84-85, 93-95]

Very often, even substances with highly efficient cytotoxic effects on cancer cells are rendered unusable for future research or eventual patient application due to an equal non-selective toxicity of the substance on healthy cells as well. Therefore, we have included a human osteoblastic cell line (hFOB1.19) in our viability experiments with the goal of observing if there is any difference in the response of healthy bone cell line to 15d-PGJ_2 and, if yes, how does this difference present itself. The hFOB1.19 osteoblast cells in particular were used as both of the OS cell lines used in your research, U2-OS and Saos-2, are of an osteoblastic origin.

Firstly, we utilized an MTT viability assay to observe the effect of 15d-PGJ_2 on our OS cell lines in a time-dependent manner. The resulting viability drop can be seen in **Figure 1**., where the viability curve showed, in an average of three separate experiments, a drop of 37% in U2-OS and 80% in Saos-2 cells after only 4 hours. After 24 h, our final treatment time point, only 16% of U2-OS and 2% of Saos-2 cells on average remained detected as viable. As an additional discovery of particular importance in the context of 15d-PGJ_2 showing promise as a potential safe anti-cancer agent, the non-malignant human osteoblastic hFOB1.19 cells showed a reduction of only 10% at the 4 h treatment time point, with 25% of the cells remaining viable after a full 24-hour treatment. These results indicated a viability that was a third higher than in the case of U2-OS cells as well as a prominent 12 times higher viability compared to the viability measured in treated Saos-2 cells.

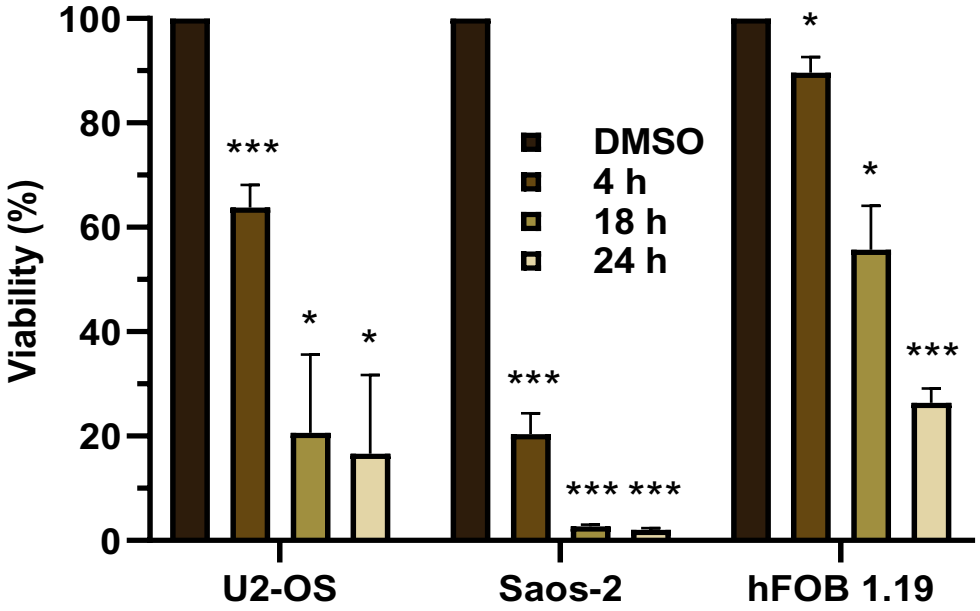

Figure 1. **15d-PGJ$_2$ negatively affects OS cell viability.** Two OS cell lines (U2-OS, Saos-2), as well as a healthy osteoblast cell line (hFOB 1.19) were treated with DMSO (vehicle control), as well as with 20 μM 15d-PGJ$_2$ for 4, 18 and 24 hours. Following this, the cells were incubated with the 2,5-diphenyl-2H-tetrazolium bromide dye, followed by a plate reader quantification of the resulting immunofluorescence color-reaction. Resulting values represent the declining cell viability within 15d-PGJ$_2$ treated OS cells in a time-dependent manner, and a significantly lower viability drop in non-malignant osteoblast cells. Means ± standard deviation are displayed. n = 3 (*P ≤ 0.05, ***P ≤ 0.005) *(reproduced from [96] with permission of MDPI publisher, Basel, Switzerland)*

In order to further investigate toxic effects of 15d-PGJ$_2$, we analyzed the microscopic morphological changes of each of the two OS cell lines, as well as the osteoblast cell line upon 15d-PGJ$_2$ treatment for 24 hours. Reduction in cell size, changes to the cell shape, as well as loss of adherence are some of the most typical signs of poor cell health, often indicating an activation of apoptosis. These findings were fitting with the effects of decreased viability observed in the MTT assay (the strongest effect being that on Saos-2 morphology). Also in line with previous results, healthy osteoblast cell line showed very minor morphological changes upon the 15d-PGJ$_2$ treatment, only displaying signs of decaying cell health after the final 24 hour treatment time point. The aforementioned microscopic effects can be seen in **Figure 2**.

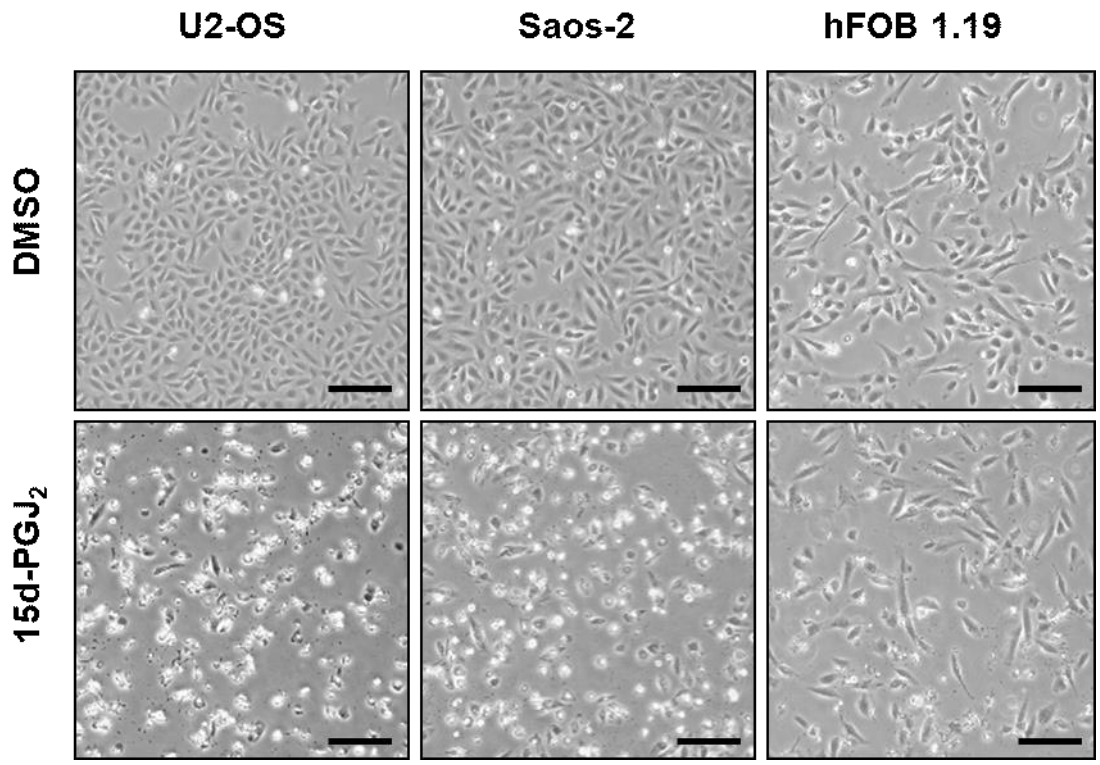

Figure 2. **15d-PGJ_2 visibly affects OS cell morphology.** OS cell lines (U2-OS, Saos-2), as well as a non-malignant osteoblast cell line (hFOB 1.19) were incubated with 15d-PGJ_2 or DMSO as a vehicle control for 24 hours. Following this, the cells were observed by light microscopy and photographed. The images show a difference between the vehicle control and the 15d-PGJ_2-treated cells, the latter showing clear signs of morphological changes indicative for cell death. Noticeable difference between the osteoblast cells and OS cells is visible. Scale bar = 500 µm. *(reproduced from [96] with permission of MDPI publisher, Basel, Switzerland).*

Exploring the inhibitory effect of 15d-PGJ_2 on OS viability further, we performed a colony-formation assay. Subsequently, as shown in **Figure 3**., this assay showed us a significant decrease in the OS cell potential to form colonies in both U2-OS and Saos-2 cell lines following a 24 hour 15d-PGJ_2 treatment. Moreover, only a scarce amount of OS cells survived in general, without showing a large capability for colony formation even after 10 (U2-OS) and 15 (Saos-2) days of culturing the cells post-treatment. These results were equally observed in every repetition, they were clearly visually present and documented. All of the aforementioned strongly indicates a significant anti-tumorigenic, anti-clonogenic potential of 15d-PGJ_2 in both OS cell lines.

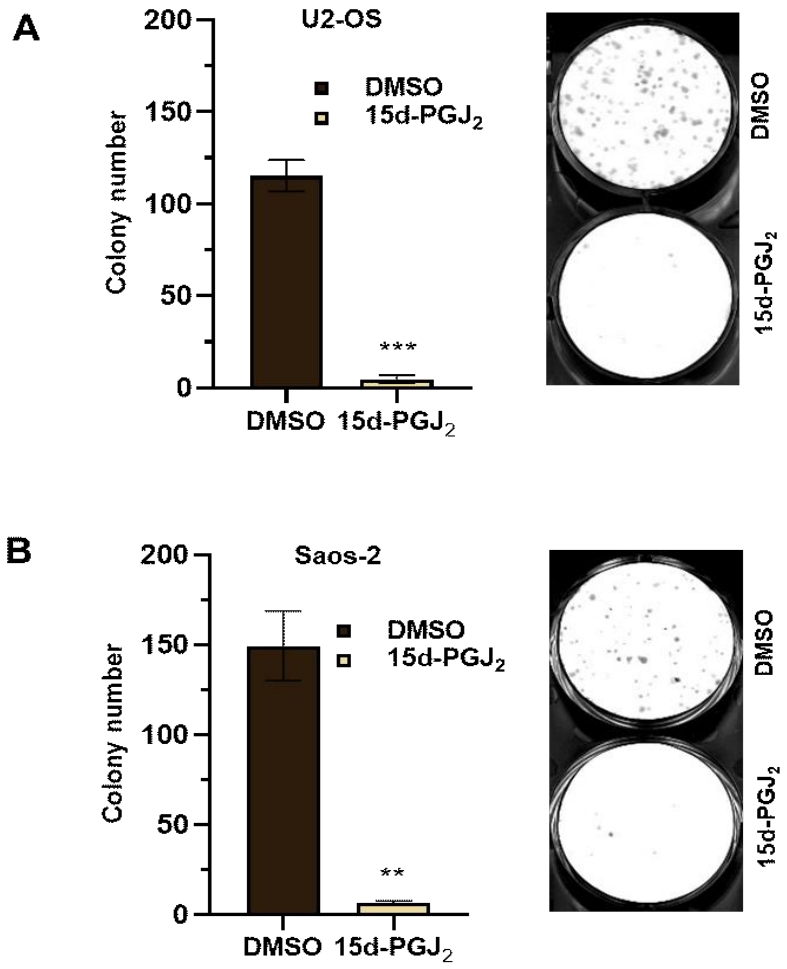

Figure 3. **15d-PGJ$_2$ negatively effects colony forming capability in OS cells.** U2-OS (**A**) and Saos-2 (**B**) cells were treated with 20 μM 15d-PGJ$_2$ or the DMSO vehicle-control for 24 hours. Afterwards, 300 U2-OS cells and 1000 Saos-2 cells from each of the group was seeded and incubated for the following 10 days in the case of U2-OS and 15 days in the case of Saos-2 cells. The formed cell-colonies were then fixated and stained with crystal violet. The images of the stained colonies were photographed and quantified via the use of ImageJ. The resulting comparison of the number of colonies of DMSO and 15d-PGJ$_2$ treated cells shows a difference and confirms a strong toxic effect of 15d-PGJ$_2$ on the colony forming ability of OS cells. Means of x independent experiments ± standard deviation are displayed. Means ± standard deviation are displayed. n = 3 (**P ≤ 0.01, ***P ≤ 0.005) *(reproduced from [96] with permission of MDPI publisher, Basel, Switzerland)*

Another cell property indicating the cell viability status is cell motility, which was our next research topic. In order to explore the effect of 15d-PGJ_2 on OS cell motility, we performed a wound healing (scratch) assay. Further fitting with our data up to this point, the resulting wound healing assay data showed a clear existence of a cytotoxic effect by 15d-PGJ_2 on both U2-OS and Saos-2 cell lines. Compared with untreated U2-OS and Saos-2 cells, the 15d-PGJ_2-treated cells visibly maintained a similar scratch width through all three observed time-points. 15d-PGJ_2-treated cells also showed a somewhat more preserved shape of scratch borders with less viable cells migrating into the empty scratch area, indicating that the cell migration was impacted as well. Both of these observations can be visible in **Figure 4.A** for the results in U2-OS cells and **Figure 4.B** for observed Saos-2 cells. The initially measured negative impact of 15d-PGJ_2 on cell viability could easily also cause such attenuation in cell proliferation and, partially, cell motility as well, resulting in the inability of the OS cells to migrate and reproduce in order to fill in the scratch area, which is an effect continuously evident in both OS cell lines.

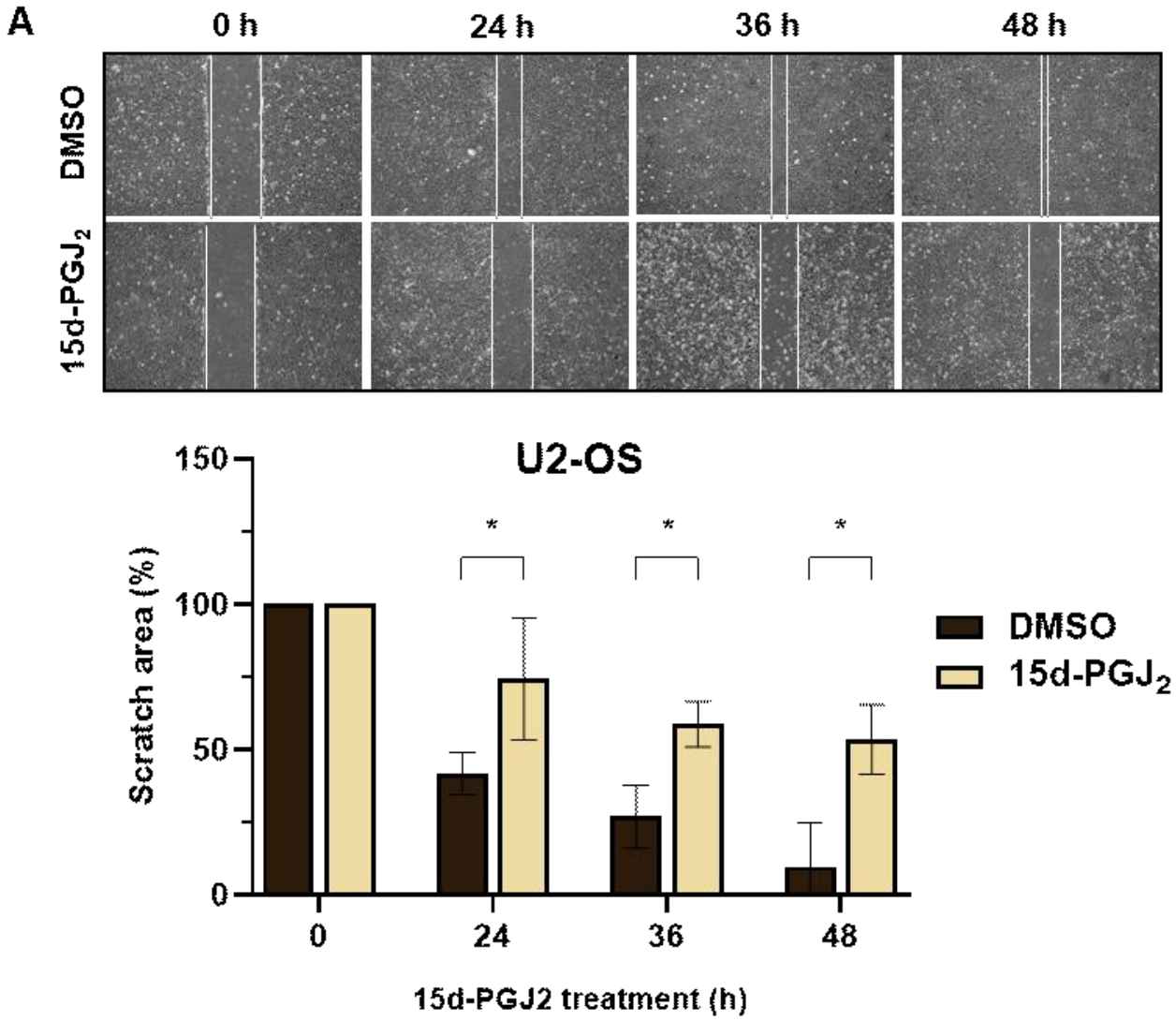
A
0 h
24 h
36 h
48 h
DMSO
15d-PGJ2
U2-OS
150
100
50
0
Scratch area (%)
*
*
*
0
24
36
48
15d-PGJ2 treatment (h)
DMSO
15d-PGJ2

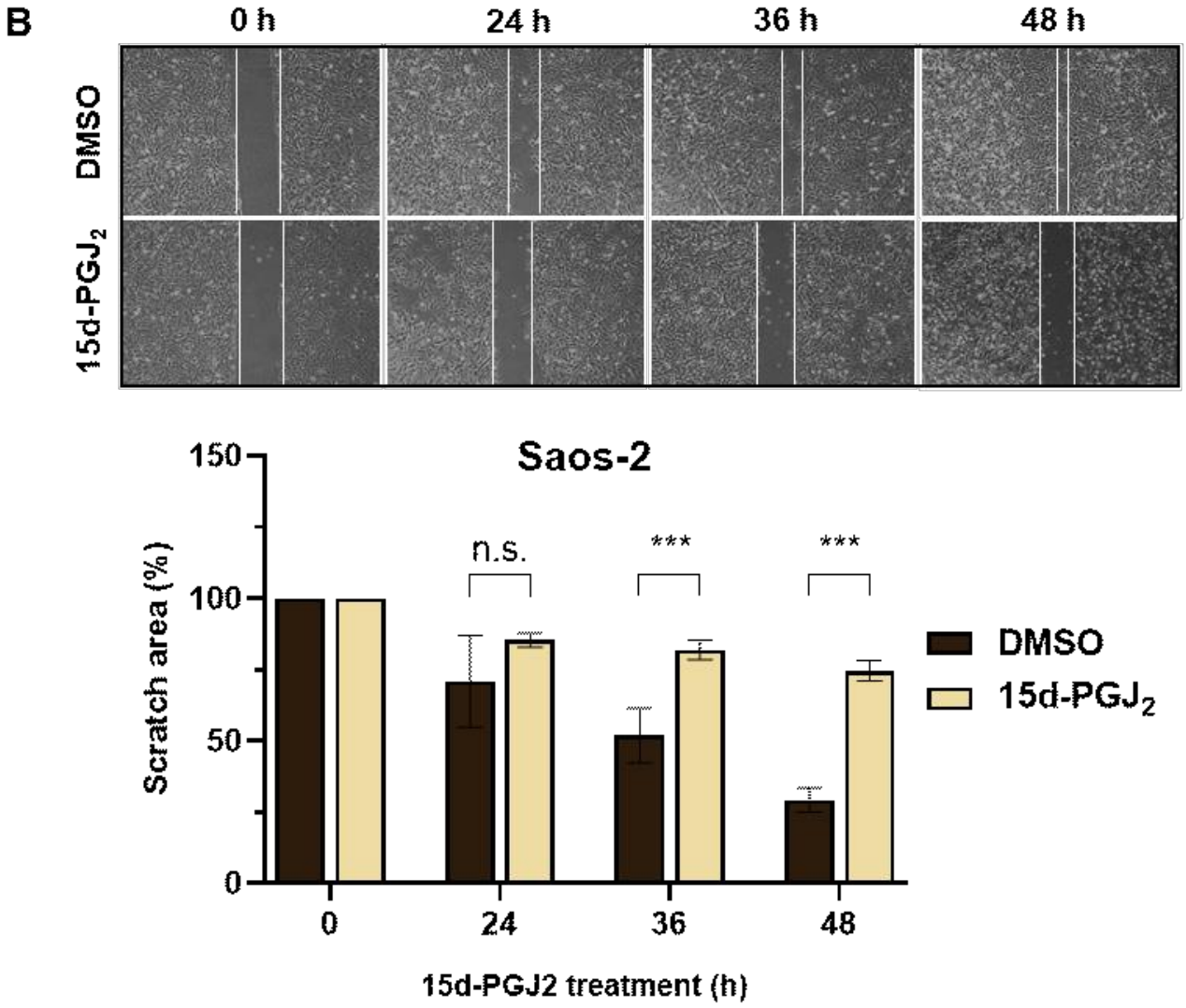

Figure 4. **15d-PGJ$_2$ negatively effects the OS cell motility and survival.** U2-OS (**A**) and Saos-2 (**B**) cells were grown until full confluence. Afterwards, the cells were treated wither with the DMSO as a vehicle-control or the 20 μM 15d-PGJ$_2$ for 24, 36 and 48 hours. The cells were continuously photographed, the scratch width measured and results quantified, displaying a significantly less reduced scratch width in 15d-PGJ$_2$ cells. Means ± standard deviation are displayed. n = 3 (*P ≤ 0.05, ***P ≤ 0.005, n.s. = non-significant) *(reproduced from [96] with permission of MDPI publisher, Basel, Switzerland)*

3.2. 15d-PGJ_2-induced ROS production in OS cells can be inhibited by specific ROS inhibitors

Due to the key role of ROS in many anti-cancer mechanisms, exploring ROS levels and potential role of ROS in 15d-PGJ_2-treated cells was our next step. It has been previously reported by our group [91] that 15d-PJG_2 successfully increased ROS production in MG-63 cells (a cell line in which 15d-PGJ_2 more prominently activated a cytoprotective mechanism rather than a solely cytotoxic one). - In order to investigate the ROS status in U2-OS and Saos-2 cells upon the earliest stages of 15d-PGJ_2 treatment, we used a specific fluorescent dye known to react in the presence of intracellular ROS. Our results showed the significant impact of 15d-PGJ_2 on the intracellular ROS levels in U2-OS (**Figure 5.A**) as well as Saos-2 cells (**Figure 5.B**). The measured increase in ROS production indicated a rise in intracellular ROS production levels with prolonged 15d-PGJ_2 treatment in OS cells. The increase of ROS production was already marked at the first time point of only 1 minute and was continued until the final observed time point of 15 minutes. This shows that the increased ROS production in OS cells is not only evidently caused by 15d-PGJ_2, but is also an example of one of the earliest mechanisms triggered intracellularly by this compound, namely, within less than minutes of the OS cells exposure to 15d-PGJ_2.

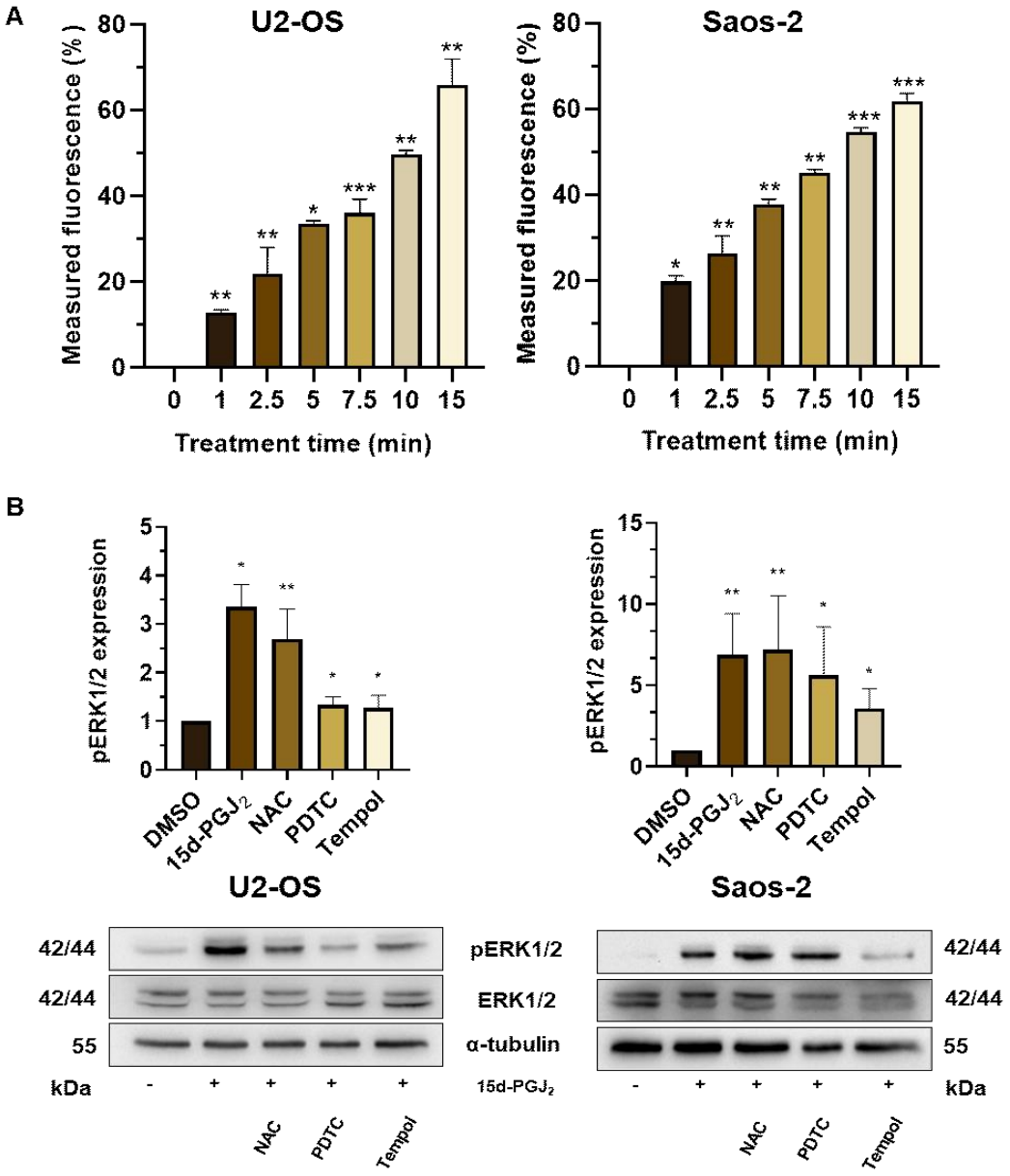

Figure 5. **15d-PGJ$_2$ causes an increase of intracellular ROS production in OS cells.** OS cells were treated with 20 μM 15d-PGJ$_2$ for time periods of 1, 2.5, 5, 7.5, 10 and 15 minutes (an untreated control was also used). Following this, ROS levels were measured within the OS cells by incubating cells with a ROS-reactive dye (DCFDA) and measuring the resulting immunofluorescent reaction. The increasing ROS activation is visible in both U2-OS and Saos-2 cell line (**A**). The effect of the measured ROS activation was observed by treating the OS cells for 15 minutes with 20 μM 15d-PGJ$_2$, along with three ROS scavengers (NAC, PDTC, Tempol) (**B**). Means ± standard deviation are displayed. n = 3 (*P ≤ 0.05, **P ≤ 0.01, ***P ≤ 0.005) *(reproduced from [96] with permission of MDPI publisher, Basel, Switzerland)*

Following this finding, we then focused on elucidating the potential effect of the increased ROS levels on other intracellular pathways, which may have been triggered. An example of another commonly early-triggered intracellular mechanism in cancer cells when treated by varying cytotoxic substances is the activation of the MAPK pathway [91].

The assessment of ROS increase effecting the activation status of MAPKs within the treated OS cells was done by checking the phosphorylation status of one of the most prominent MAP kinases, the extracellular signal-regulated kinase (ERK1/2, also commonly known as p42/44 MAPK). As our ROS results displayed a prominent increased ROS level within both OS cell lines already after 15 minutes, we used this time point to observe the effect 15d-PGJ_2 on the ERK phosphorylation with and without pre-treatment with the additional ROS-inhibitors. Three known ROS scavengers were used in this experiment, namely NAC (N-acetyl-cysteine, a cell permeable thiol that restores intracellular glutathione), PDTC (pyrrolidine dithiocarbamate, a metal chelating antioxidant compound) as well as Tempol (a superoxide dismutase (SOD) mimetic as well as a superoxide anion radical scavenger). As shown in Figure 5.C and 5.D, NAC slightly inhibited the phosphorylation of ERK in the U2-OS cell line, however, this wasn't noticed in Saos-2. Similarly, we observed that PDTC reduced the ERK1/2 phosphorylation in U2-OS cells, however, the effect was significantly less present in Saos-2 cells. Tempol, on the other hand, significantly weakened ERK1/2 phosphorylation in both OS cell lines.

3.3. 15d-PGJ_2 induces acute apoptosis in OS cells

Since our results so far indicated a strong impact of 15d-PGJ_2 on cell viability, it was our next intent to further clarify and confirm the induction of apoptosis in both of the OS cell lines. As we wanted to use experimental approaches that were very precise in exploring and identifying different types of cell apoptosis, we used two well-known apoptosis-identifying approaches.

The first approach was an Annexin V/PI assay following a 15d-PGJ_2 treatment lasting up to 24 hours. By using flow cytometry, one can detect cells whose phosphatidylserine had successfully bound to Annexin V antibody. The presence of this specific phospholipid on the outer plasma membrane leaflet is a clear indication of the apoptosis activation, as this shows that the cells membrane integrity, signified by the specific location of phosphatidylserine, has

already been compromised. The significance of PI staining is similar, in that PI is not able to permeate living cells and mainly binds with the cell DNA material (it is known to intercalate between DNA bases, ultimately ending up with the binding ratio of one dye molecule per 4-5 base pairs), accessible only at late stages of cell degradation and apoptosis.

We were able to elucidate a time-dependent increase of cell apoptosis in both OS cell lines treated with 15d-PGJ_2. The reaction with both Annexin V and PI confirms the presence of late apoptosis in both cell lines already at the 4-hour treatment. It is important to note that the detected apoptosis activation was somewhat weaker in U2-OS (**Figure 6.A**) cells, which resonates appropriately with the previous viability data that we have obtained. Altogether, this suggests a somewhat stronger sensitivity of the Saos-2 cell line (**Figure 6.B**) to the 15d-PGJ_2 in comparison to U2-OS cells.

In the slightly more resistant U2-OS cells, the percentage of early and late apoptotic cells was 21% after 12 hours and 33.6% after 24 hours of 15d-PGJ_2 treatment. Similar, but in slightly lower amount, were the values measured in Saos-2 cells, with 26.3% and 44% of apoptotic cells upon 12 and 24 hour of 15d-PGJ_2 treatment, respectively. Important to note is also that the percentage of cells in early apoptosis was significantly lower than those in late apoptosis, this being true for both OS cell lines and ranging from 6% to 8%. Necrotic cells were present in both cell lines, though in an even smaller percentage below 1.5%.

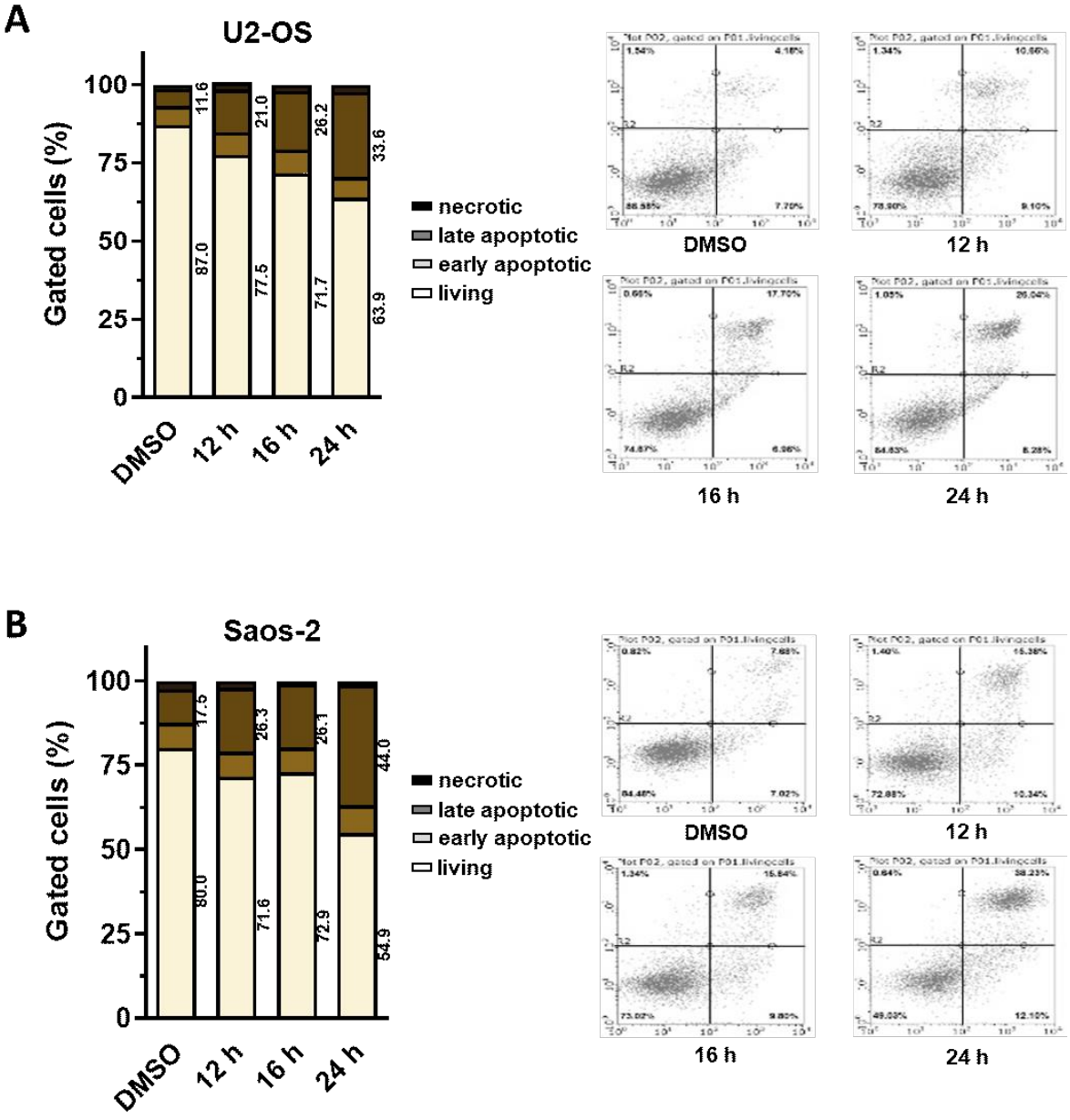

Figure 6. **15d-PGJ$_2$ activates apoptosis in OS cells.** Following a 15d-PGJ$_2$ treatment (20 μM) of OS cell lines (U2-OS, Saos-2) for 12, 16 and 24 hours, as well as a DMSO vehicle-control, the cells were additionally treated with Annexin and PI and analyzed via flow cytometry. The results show a prominent activation of apoptosis in the U2-OS cell line (**A**) with a slightly stronger effect observed in Saos-2 cells (**B**). *(reproduced from [96] with permission of MDPI publisher, Basel, Switzerland)*

To confirm the strong apoptotic effects that 15d-PGJ_2 has on OS cells, we investigated the expression of some of the most prominent protein markers of cell apoptosis, namely the cleaved form of caspase 3 and PARP (Poly-ADP ribose polymerase). When the process of apoptosis is activated, at a certain point caspase 3 is translocated to the cell nucleus where it then interacts with a variety of DNA-interacting proteins – one of them being PARP. Therefore, both of these enzymes play a crucial role in the intracellular apoptotic pathway and observing their expression/activation within cells often proves a clear confirmation of apoptosis being active and present.

Figure 7.A and **B** successfully show the marked increased expression of both cleaved-caspase 7 and PARP in both OS cell lines, as shown by western blotting. In line with our previous results, Saos-2 cells once again show a somewhat stronger apoptotic enzyme expression in 15d-PGJ_2-treated cells than U2-OS does. Both cell lines showed a strong apoptosis activation already at a 4-hour time point, further proving the strong impact of 15d-PGJ_2 on OS cells.

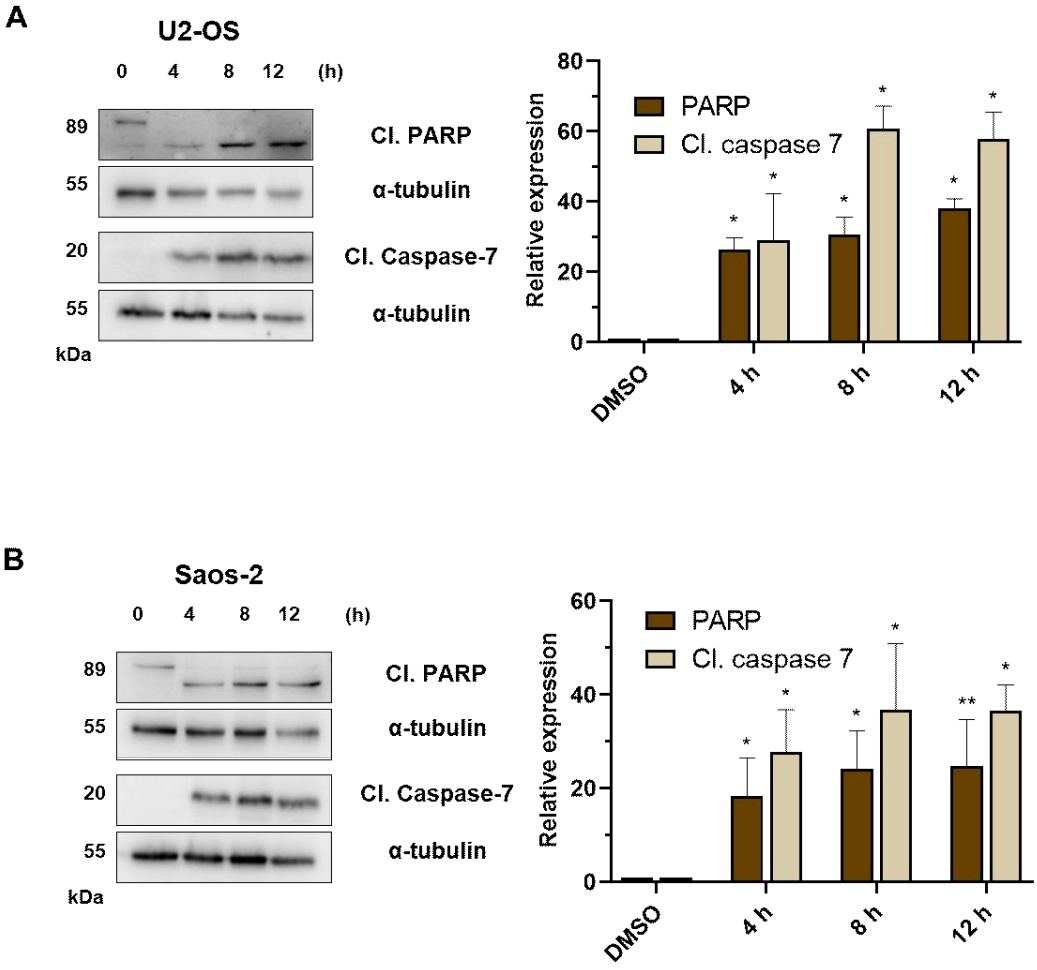

Figure 7. **15d-PGJ$_2$ induced apoptosis in OS cells is time-dependent.** U2-OS (**A**) and Saos-2 (**B***)* were treated with either a DMSO vehicle-control or 20 μM 15d-PGJ$_2$ for 4, 8 and 12 hours. The resulting effects on intracellular protein expression were then visualised via western blot and appropriately quantified. The obtained results show a time-dependent growth in expression of the cleaved versions of apoptosis-specific proteins PARP and Caspase-7 in both of the OS cell lines. Means ± standard deviation are displayed. n = 3 (*P ≤ 0.05) (*reproduced from [96] wit*h permission of MDPI publisher, *Basel, Switzerland)*

3.4. The importance of 9,10 carbon double bond in 15d-PGJ_2 effect on U2-OS and Saos-2 cells

Our previous data with the MG-63 cell line indicated a strong, prerequisite-type role of the double bonded C9 atom in the molecular structure of 15d-PGJ_2 in causing its particular cytotoxic effects on the cells. Because of how different, both genetically and on a molecular level, all of these three OS cell lines are compared to one another, we were curious to see if this part of the 15d-PGJ_2 molecular structure also plays an important role in U2-OS and Saos-2 cell lines.

In order to confirm this, we treated U2-OS and Saos-2 cells with a 15d-PGJ_2 analogue in a method similar to the one used in the previously described apoptosis-confirming time kinetic experiment. However, in this case, we only focused on one single later time-point that has shown clear apoptosis enzyme activation in our previous experiment (12 h). Both of OS cell lines were treated, with either 15d-PGJ_2 or its analogue lacking the aforementioned carbon atom C9 (9,10-dehydro-15d-PGJ_2). The results of these experiments confirmed the strong effects of 15d-PGJ_2 in terms of apoptosis activation within both OS cell lines, however it also demonstrated a clear, visible lack of any similar effect when the cells were treated with the 15d-PGJ_2 analogue. With these findings, we can therefore confirm that, similar to the previous findings in MG-63, the specific C9 carbon atom in the lipid's molecule truly does yet again play a crucial role in 15d-PGJ_2 administering its cytotoxic effects within the U2-OS and Saos-2 cell lines (**Figure 8**).

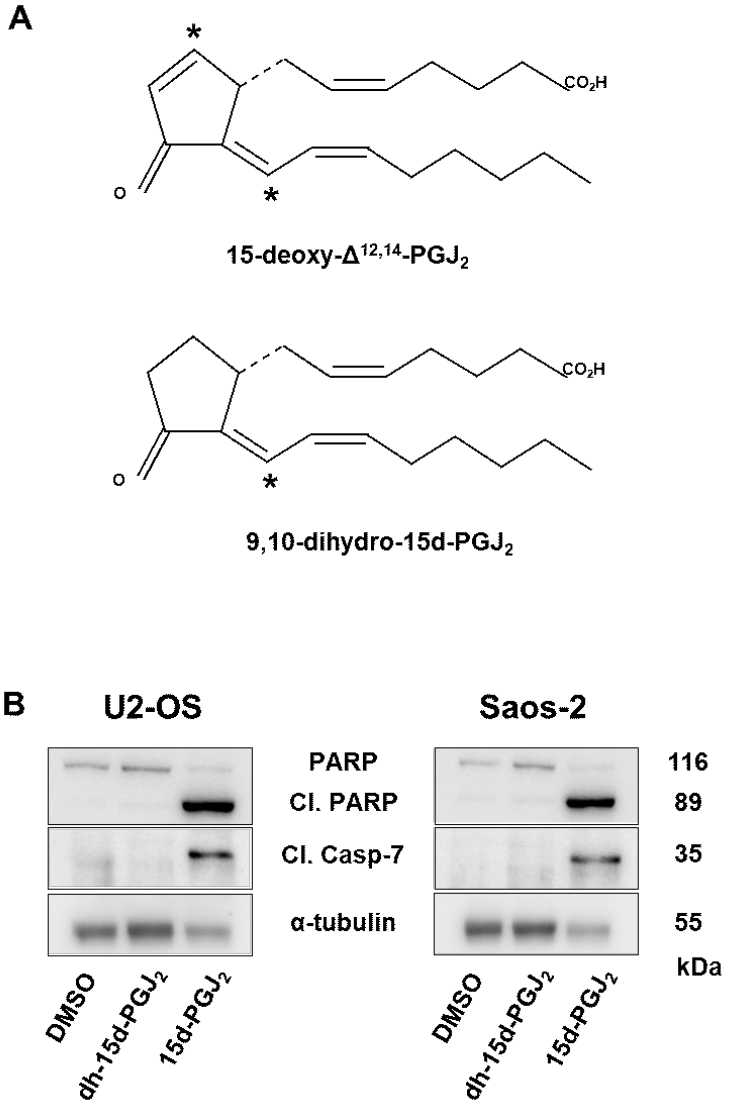

Figure 8. **9,10-dh-15d-PGJ$_2$, a structural analogue of 15d-PGJ$_2$ lacking the electrophilic carbon atom C9, is crucial for the compound's effect on OS cells.** OS cells (U2-OS and Saos-2) were treated with 20 μM 15d-PGJ$_2$ (**A**) and 9,10-dh-15d-PGJ$_2$ (**B**) separately for 12 hours. Following this, the expression of pro-apoptotic proteins in the cell lines, namely cleaved-PARP and cleaved-caspase 7, was analyzed via western blot and appropriately quantified. Results show a lack of apoptosis activation in cells treated with the analogue. This data confirms the crucial role of the C9 double bond present in the structure of the 15d-PGJ$_2$ molecule. Representative images from 3 independent experiments were used. *(reproduced from [96] with permission of MDPI publisher, Basel, Switzerland)*

3.5. 15d-PGJ_2 induces time-dependent MAPK activation in OS cells

MAP kinase pathway is one of several known protein pathways that may be activated during the beginning of cytotoxic events triggered in cancer cells. [57] In order to follow up with these findings, we decided to do a more detailed time kinetic-based series of experiments lasting up until the 1-hour time point.

To analyze the behavior of the aforementioned MAPK proteins after 15d-PGJ_2 treatment, we detected the phosphorylated (i.e. activated) versions of ERK1/2, p38 MAPK and c-Jun N-terminal kinase (JNK) proteins. Our results indicate a clear trend of time-dependent increase of phosphorylation for all three proteins in both the U2-OS and Saos-2 cell lines, as shown in Figure 9.

These findings indicate a continuous and rapid activation of the MAPK pathway on the level of all three tested proteins (ERK1/2, p38 and JNK) within OS cells, triggered by 15d-PGJ_2.

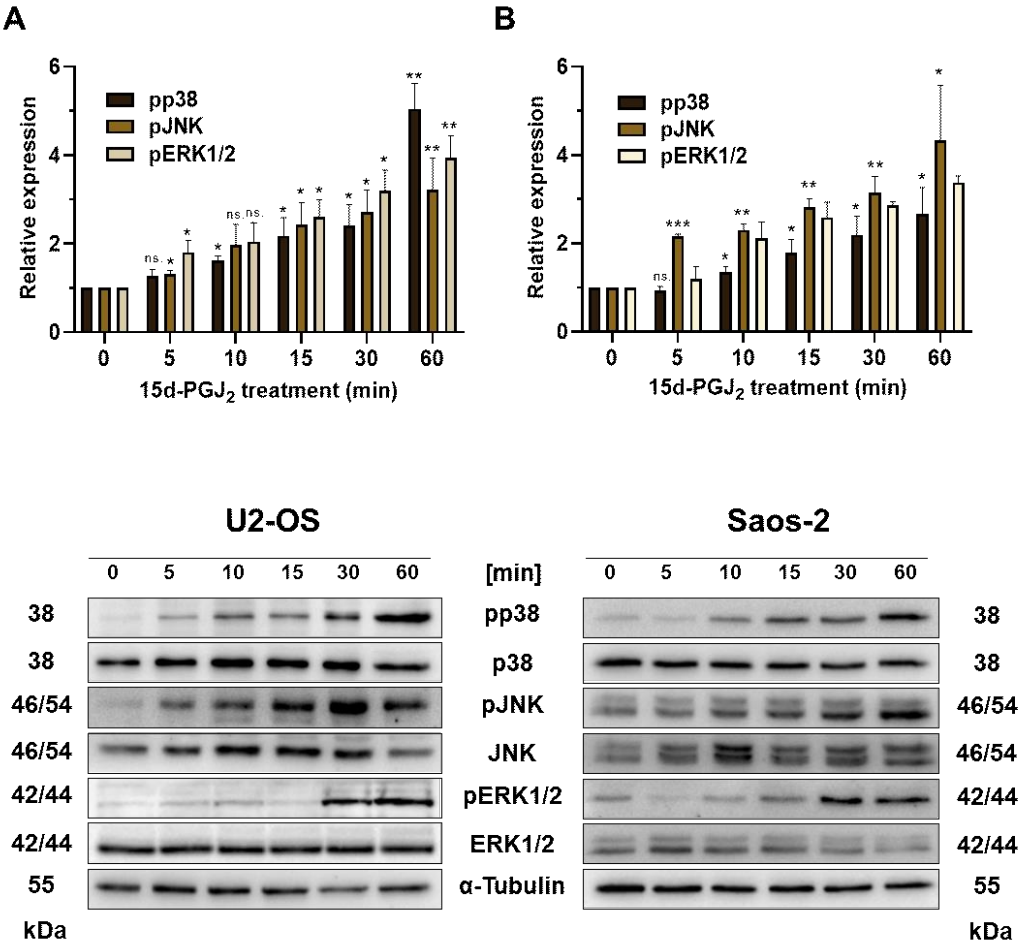

Figure 9. **15d-PGJ$_2$ activated the MAPK pathway in OS cells.** After treating the OS cells (U2-OS and Saos-2) with 15d-PGJ$_2$ (20 μM) for 5, 10, 15, 30 and 60 minutes, as well as with a DMSO vehicle control (marked as '0'), the activation of MAPKS, namely, pp38, JNK and ERK1/2, via western blot was observed. These results were quantified and indicated a time-dependent increase in the MAPK activation triggered by the 15d-PGJ$_2$ treatment. This effect was present in both the U2-OS (**A**) as well as Saos-2 (**B**) cell line. Means ± standard deviation are displayed. n = 3 (*P ≤ 0.05, *P ≤ 0.01, *P ≤ 0.005, n.s. = non-significant) *(reproduced from [96] with permission of MDPI publisher, Basel, Switzerland)*

3.6. The cytotoxic effect of the 15d-PGJ_2 treatment fails to trigger any significant cellular defense mechanisms

Based on the findings of our previous work with 15d-PGJ_2 and the MG-63 cell line [91], we wanted to check whether there would be any sort of an antioxidative cell-defense mechanism happening simultaneously to the cytotoxic events in U2-OS and Saos-2 OS cell lines which are genetically and morphologically different from MG-63. In order to do this, we next preformed a longer time kinetic-based experiment, with treatments lasting up until 8 hours. The results showed an eventual decrease in expression of several known antioxidant-acting proteins, namely, the zinc-finger transcription factor early growth response factor (Egr1), basic leucine zipper transcription factor nuclear factor E2-related factor 2 (Nrf2), nuclear factor NF-kappa B (NF-κB), as well as the activated/phosphorylated version of the AKT enzyme. The resulting data suggest, as shown in Figure 11, that Nrf2, as well as NF-kB had been in a steady decline from the very beginning of 15d-PGJ_2 treatment of the OS cells. EGR1 decreased continually after slight increase at the 1-hour time point. AKT presented a slightly different behavior, namely in the fact that it showed a much stronger increased phosphorylation at the 1st and 2nd hour of treatment, however, already at 4 hours this expression was reduced and continued to decrease, rendering the activation insignificant for the ultimate fate of the cells.

Ultimately, we can conclude that no cytoprotective mechanism are occurring at a significant level in either of our cell lines treated with 15d-PGJ_2.

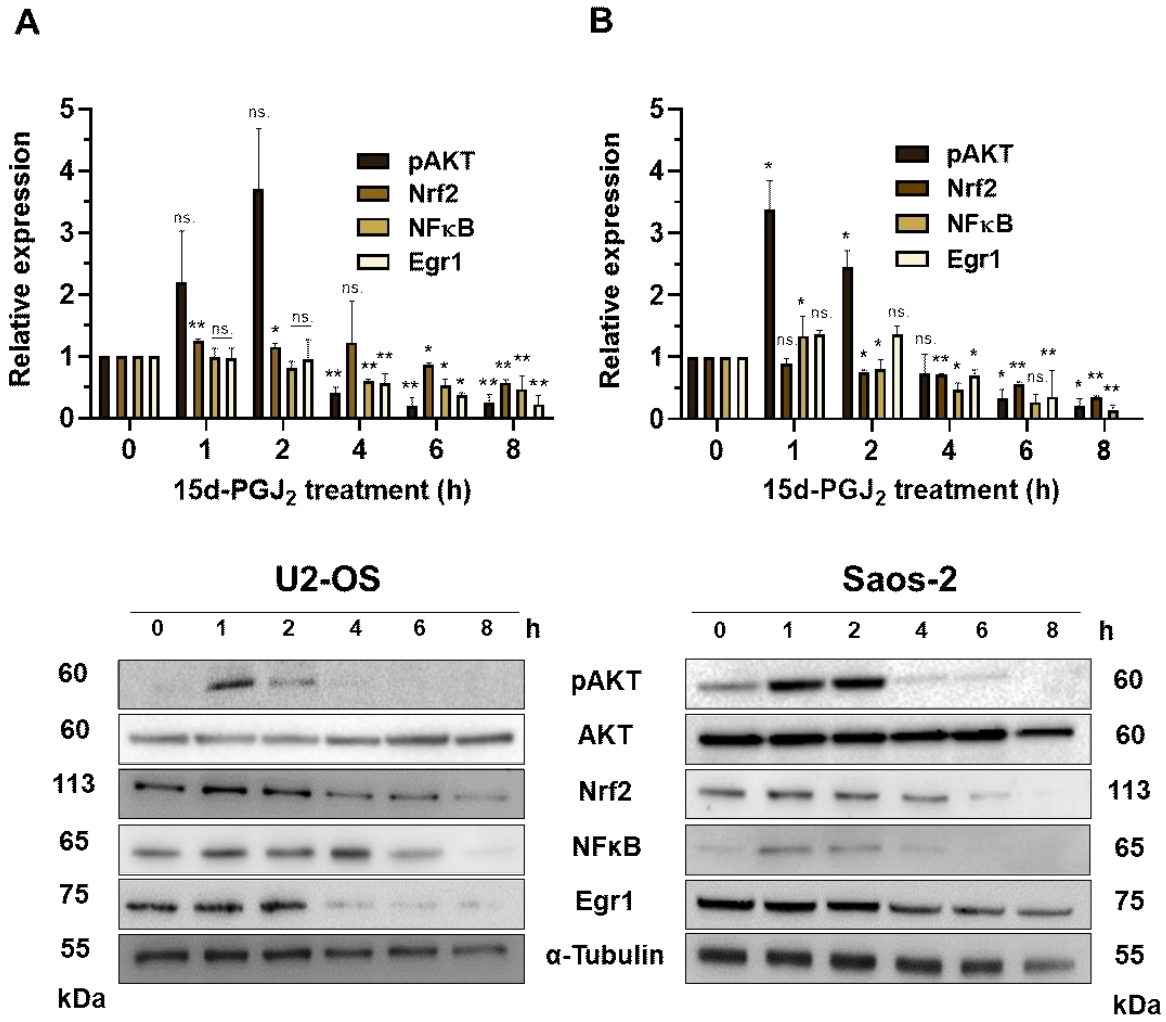

Figure 10. **15d-PGJ$_2$ fails to activate any significant cytoprotective mechanisms in OS cells.** OS cells (both U2-OS and Saos-2) were treated with 20 μM 15d-PGJ$_2$ for 1, 2, 4, 6 and 8 hours, as well as a DMSO vehicle control. Afterwards, we analyzed the effects this had on the two cell lines by visualizing the expression of several proteins often known for facilitating cytoprotective mechanisms (pAKT, Nrf2, NFkB, Egr1). The results indicated that the expression of all of the aforementioned proteins drastically declined, indicating a lack of a protective mechanism enhanced by them. This was observed in similar manner in both U2-OS (**A**) and Saos-2 (**B**) cell lines. Means ± standard deviation are displayed. n = 3 (*P ≤ 0.05, **P ≤ 0.01, n.s. = non-significant) *(reproduced from [96] with permission of MDPI publisher, Basel, Switzerland)*

3.7. 15d-PGJ$_2$ inhibits OS tumor growth in the CAM model

In vivo animal models have been a challenging topic when it comes to OS research. An *in vivo* model that is unanimously functioning when it comes to these two cell lines must be established yet, as the present *in vivo* experiments are still somewhat sparse and non-conclusive. Some of the published work, where *in vivo* models were used, mainly include the process of xenografting human patient-derived tumor tissues into mice, while cell-based *in vivo* results feature only several examples of intraperitoneal injection procedures with varying success.

However, there are several other methods, which might help bridge this span from *in vitro* to *in vivo*. One of these methods is the chicken chorioalantoic membrane (CAM) assay, an reliable approach that uses the membrane of a living and developing chicken embryo as a growing and observational ground for various types of cells. In order to have a comparative point of how the growth of an already researched type of OS would develop on CAM versus how our two OS cell lines behave, we used MG-63 as an additional cell line used and tested in this model of experiment. Within each cell line, we performed the comparison between cells onplanted on the membrane that were treated with either our vehicle compound (DMSO) or with 15d-PGJ$_2$. After allowing the cells to grow on the membranes of young chicken embryos for three days, the growth of onplants was photographed and analyzed.

Already at the level of macroscopic as well as microscopic observation of the onplant growth, it was evident that the cells treated with 15d-PGJ$_2$ prior to the onplanting showed a visibly lower level of growth and thriving compared to growth of cells treated with DMSO. While the vehicle-treated cells showed typical tumor growth and tumor cell behavior and developed already after three days of incubation, the treated cells formed much smaller tumors, often lacking the strongly defined form of the growths that the vehicle-treated cells had, most prominently in U2-OS cells. This can be seen in **Figure 11**.

Immunohistochemical analyses via hematoxylin-eosin (HE) staining additionally confirmed the smaller number of cells within treated cell growths. Also noticeable already at the HE-basis was the generally much smaller groups of cells having a viable, typical OS cell morphology within the growth tissues containing 15d-PGJ$_2$ treated cells.

The next step was analyzing the expression of Ki-67, a well-known proliferation marker on the stained tumor tissue. These results further confirmed our data showing less pronounced proliferation of 15d-PGJ$_2$ treated cells, vs. DMSO treated cells. Taken altogether, this data strongly fits with the information gathered thus far in our previous experimental approaches,

additionally validating the conclusion that 15d-PGJ_2 has a remarkable cytotoxic effect on OS cells.

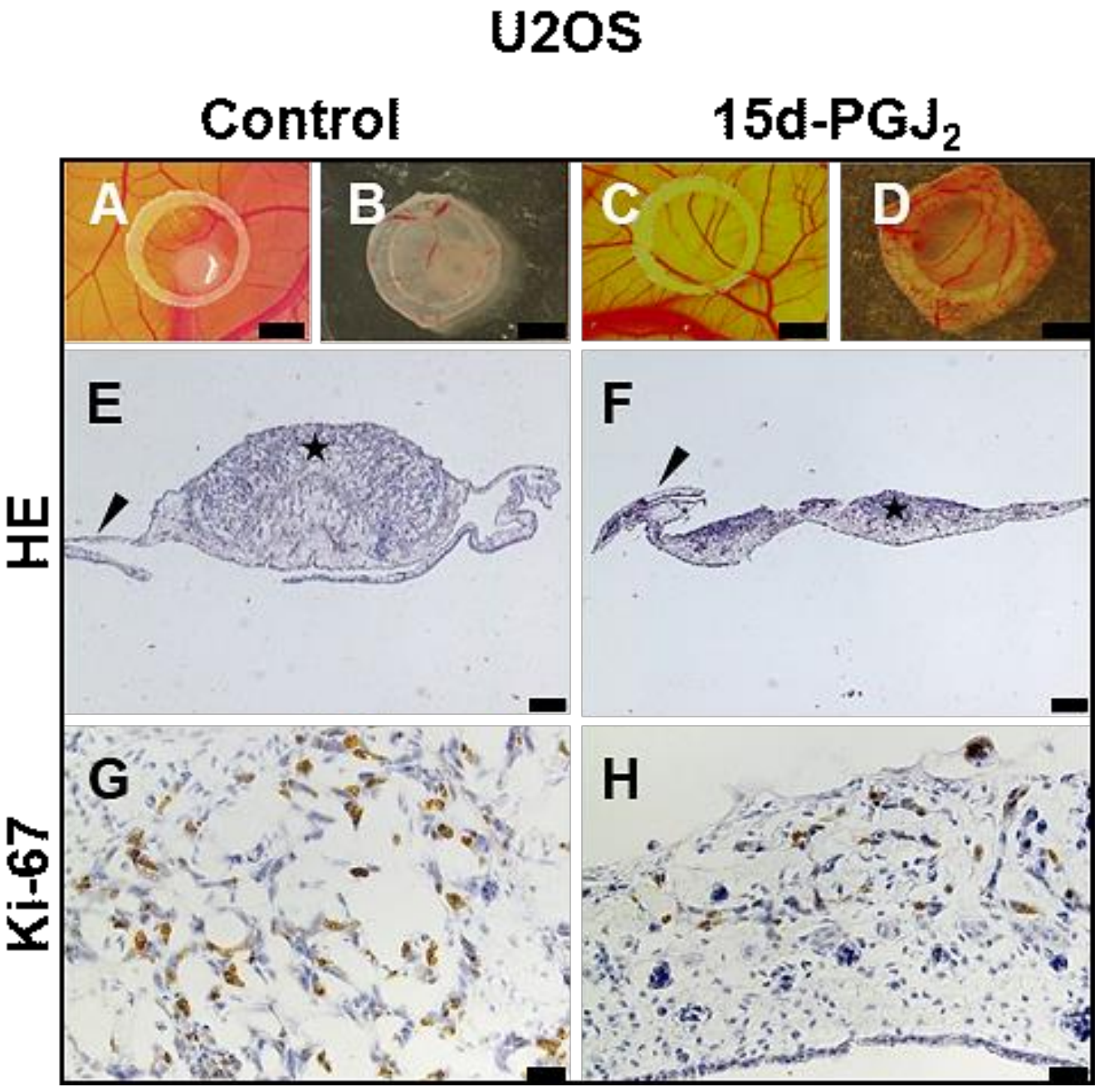

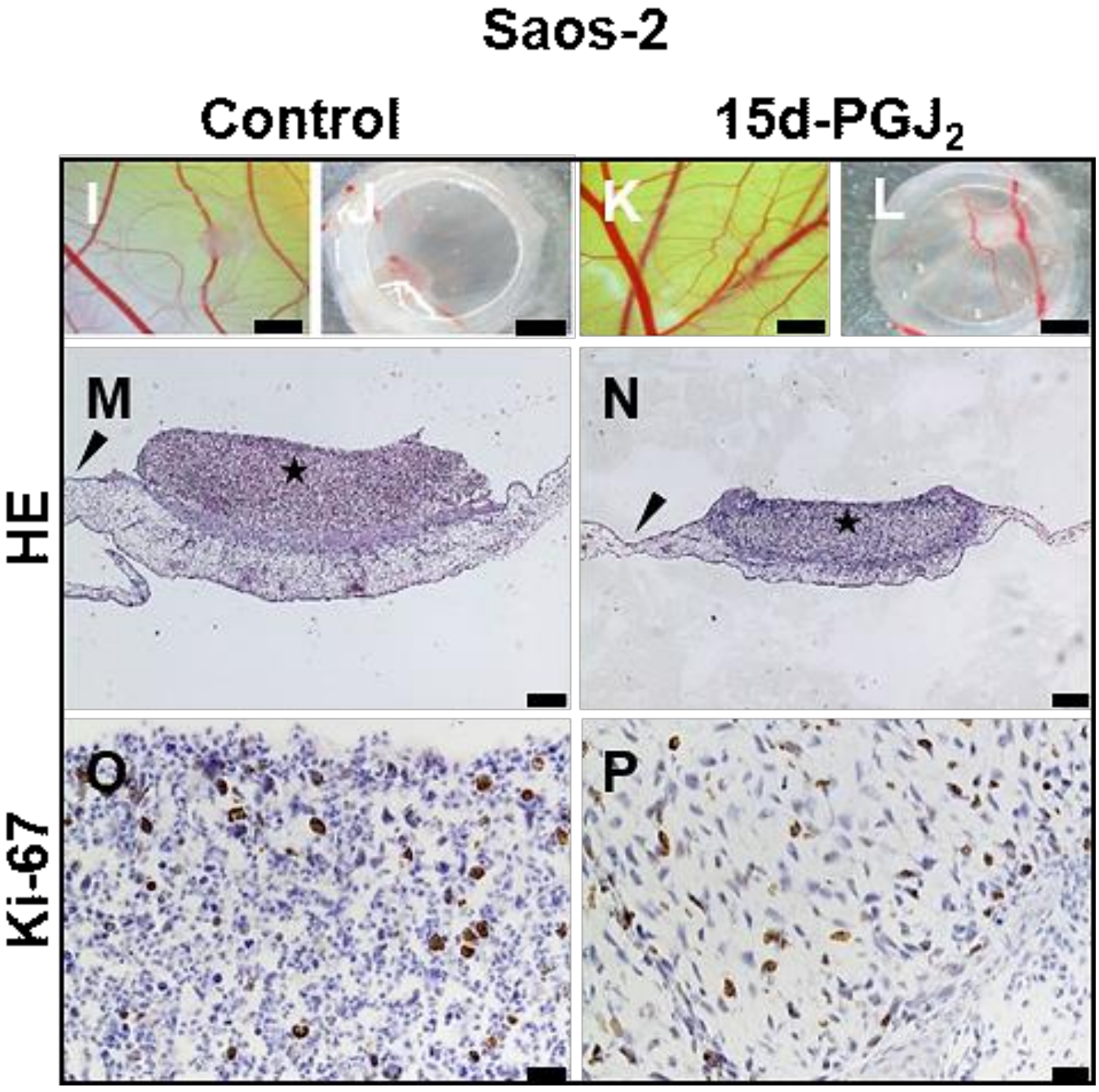
Saos-2
Control
15d-PGJ2
I
J
K
L
M
N
O
P
HE
Ki-67

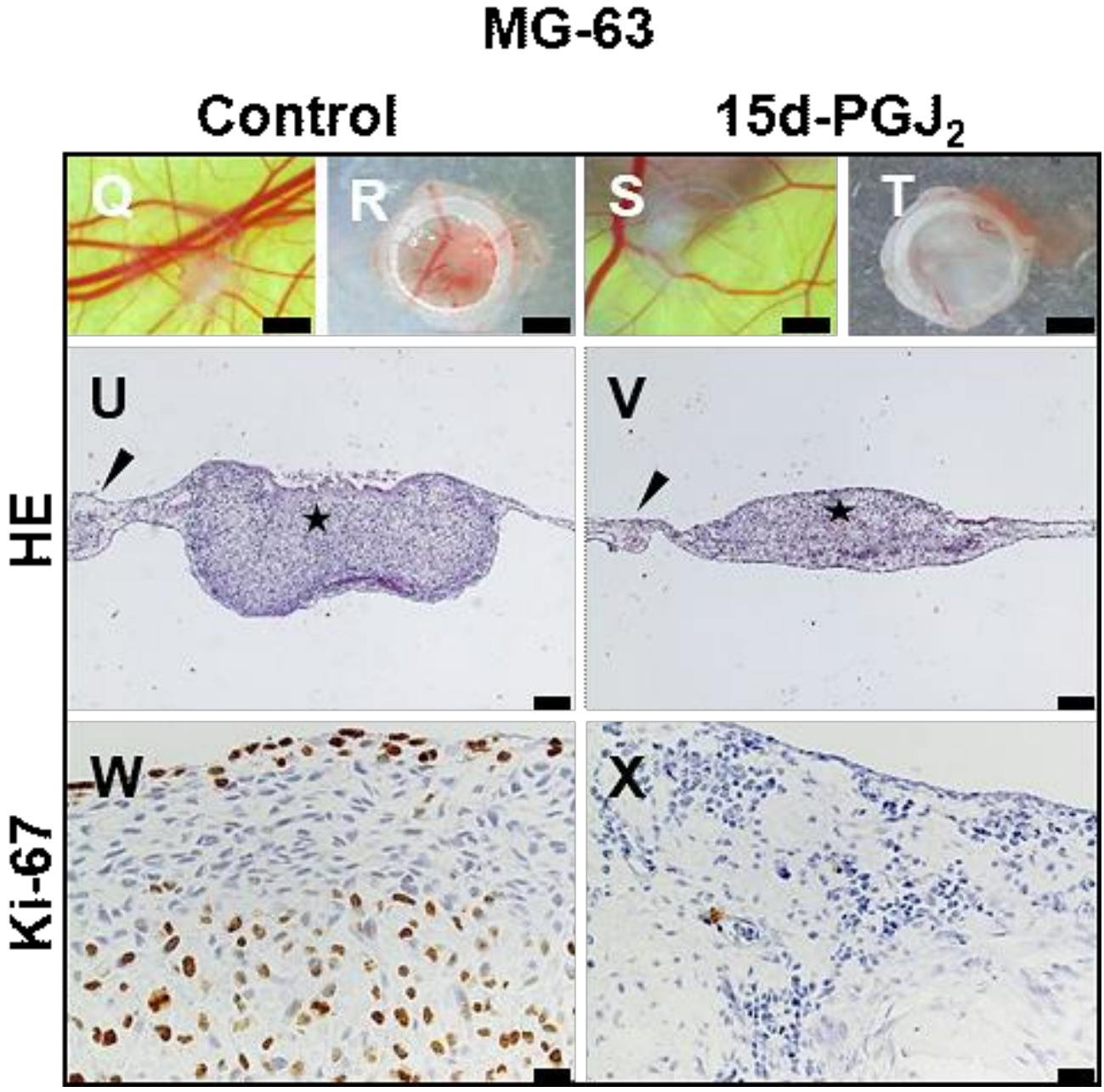
MG-63
Control
15d-PGJ2
Q
R
S
T
U
V
HE
W
X
Ki-67

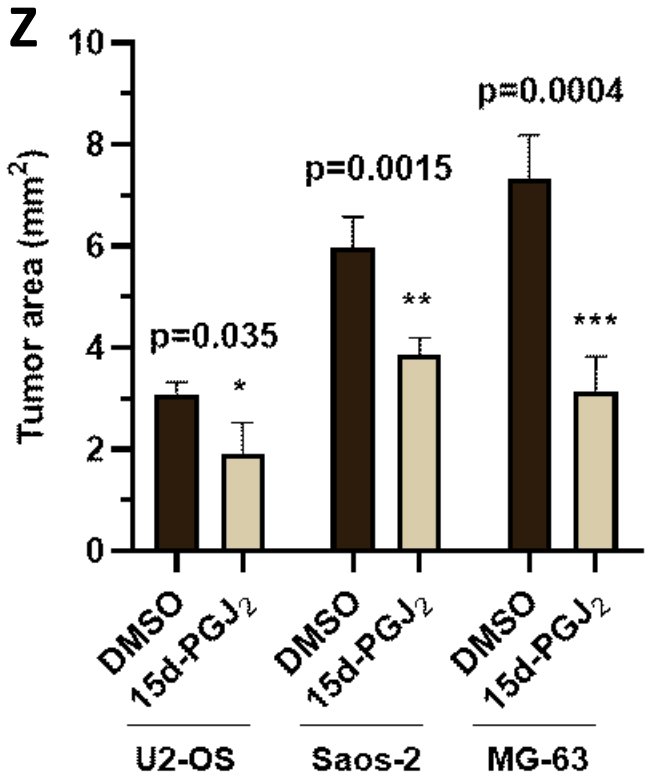

Figure 11. **15d-PGJ$_2$ shows effects on CAM onplanted OS cells.** Following a 3 day incubation period of both DMSO and 15d-PGJ$_2$ (20 µM) treated OS cells (U2-OS, Saos-2, and MG-63), onplants were photographed, excised and prepared into histological samples for further analysis. Onplant photography shows a significant difference in the onplant size of 15d-PGJ$_2$-treated vs. controls, with cell density also appearing higher in control cells (**A-D**, **I-L**, **Q-T**). The onplant growth was quantified via ImageJ tumor area measurement. (Z) Immunohistochemical analysis of the onplant structure confirmed the difference in size and cell density (**E-F**, **M-N**, **U-V**). The Ki-67 staining also indicated a difference in cell proliferation in all three cell lines: U2-OS (**G-H**), Saos-2 (**O-P**) and MG-63 (**W-X**). Means of five different onplants per group ± standard deviation are displayed. (*P ≤ 0.05, **P ≤ 0.01, n.s. = non-significant) *(reproduced from [96] with permission of MDPI publisher, Basel, Switzerland)*

4. DISCUSSION

Among a variety of bone cancer subtypes, OS is the most common and it most often affects children and adolescents [1-4]. Other than the fact that it most commonly affects the youngest demographic, another prominent problematic of OS is its difficulty of diagnosis in the early stages of the illness due to very discreet and misleading symptoms, especially in young and adolescent patients (i.e., mild joint pain, bruises and light swelling on affected area). Very often, this results in the diagnosis being made at later stages of the cancer progression when the tumor progressed into metastases, most commonly within the lungs as the initial secondary location of the tumor [2-4]. The existing therapy for OS is surgical removal (occasionally including amputation or excision of affected limbs or areas), chemotherapy and radiotherapy. The latter two pose a unique threat to the younger patient demographic due to their propensity for causing long-term side-affects. Because of this, finding the appropriate therapy that can efficiently and quickly tackle the cancer progression without harming the mostly young patients with potentially harmful long-term side-effects is the current main priority in general OS research. Currently, the most effective method of repressing the cancer growth at the stages where the main OS lesion has started spreading is the aforementioned method of amputation. Chemotherapy is often used for post-surgical treatment, as well as in the cases of patients suffering from later stages of the illness, however, the toxicity of the currently commonly used chemotherapeutics (considering the often very young age and higher body sensitivity of the patients) does not increase the therapy success rate enough to show any of these therapeutics as sufficiently safe and efficient [27-29].

Certain progress has been made in pharmaceutical research with drugs such as trabectedin and irinotecan [97-98]. These drugs have shown a promising potential in the quest for refining safer and more effective OS chemotherapeutics. Their improval in target specificity is achieved via their capability of interacting only with specific DNA regions within the tumor microenvironment and initiating their effects there. Trabectedin is currently actively used as one of possible anti-sarcoma chemotherapeutics in Europe, Russia and South Korea, while irinotecan is used throughout the world, though it was initially only used for colon cancer and small cell lung carcinoma treatment and is only being investigated for its potential use in OS in the past several years. However, as promising as their mechanisms of action are, as well as how positive some of the patient reports are in regards to treatments with these types of chemotherapeutic, the ratio of toxicity versus efficiency of these drugs (while somewhat better in comparison to the chemical therapeutics currently used, i.e. doxorubicin, cisplatin, methotrexate) still remains reasonably unfavorable and unfortunately far from ideal. The

greatest issue in the cases of similar synthetic drugs remains the lack of complete selection precision of the targets of these chemotherapeutics, where even their seemingly highly selective methods of cell targeting and destruction can show error, as notable by the still present reported side effects [97, 98]. In the context of these issues, focusing on more natural substances that harm the cancer cells while at least somewhat sparing the surrounding tissue as well as the general body metabolism, presents a potentially better approach to future therapies.

Cyclopentenone prostaglandins have been widely investigated for their prominent anti-inflammatory properties for almost three decades, with emphasis on its potent capabilities of stifling the immune response on its various levels and in a variety of immunological states and responses [52-55]. The research into their anti-cancer capabilities, however, had started fairly more recently, mostly within the past ten years, where it has shown promising anti-cancer effects in cell and animal models of breast cancer, prostate cancer and colon cancer, among several other examples [43, 64-65]. Therefore, it can be said that even in regards of the their effects in an oncological context, these effects of prostaglandins (mainly PGD2 and PGE2) have been proven on a basic level in a wide variety of tissues, serving as fertile ground for further research into its anti-tumorigenic properties. However, even though the effects of several prostaglandin compounds have been observed in a great number of tissues and cancers, the exact cellular mechanisms of these effects have not been fully elucidated yet. This presents itself as a huge gap that still remains in regards of research related to several types of prostaglandins and their potential anti-tumorigenic properties, a gap that urgently needs to be filled in order to unveil crucial biomedical data necessary for any of the prostanoid compounds to continue advancing towards a possible role of an anti-cancer therapeutic.

Another example of the more frequently investigated prostaglandins in terms of its anti-cancer effects is 15d-PGJ_2 – one of the final products of an unsaturated omega-6 fatty acid, the arachidonic acid. One of the appealing and intriguing characteristics of 15d-PGJ_2 as an anti-tumorigenic agent is that it is in fact a naturally occurring substance, already present in the human bodily fluids such as the serum and plasma, though it is also confirmed to be excreted via urine. Under conditions of stress or inflammation, its concentration rapidly increases [59, 99]. Due to the fact that finding a substance that harms the OS cancer cells but spares the surrounding healthy tissue (as well as the general bodily system) while retaining its vigilant toxicity towards any malignancies present, it is highly promising that our results show a significantly smaller cytotoxic impact of 15d-PGJ_2 on the treated non-malignant osteoblast cells as compared to both OS cell lines used (U2-OS and Saos-2), both in

morphologically and in terms of its effect on cell viability and apoptosis. Seeing as our cells are that of an osteoblastic origin, this serves as particularly optimal groundwork for further planning of similar experiments where both malignant and healthy cells could be tested, optimally in an animal model.

These results also show a promising aspect of 15d-PGJ_2 as a potential therapeutic agent in the context where most anti-tumorigenic substances currently used in cancer therapy are not only artificially synthesized but can also, as previously mentioned, be highly toxic to the human body even at lower levels [12-15]. Considering these facts, 15d-PGJ_2, as a naturally present compound, could potentially serve as a safer alternative. The necessity in this regard would be to create a more detailed analysis of the concentrations of 15d-PGJ_2 that a body could safely endure and maintain without causing damage to healthy surrounding tissues at the same time as it causes damage to the tumorigenic ones. Secondly, this could lead to the need of finding a method of successfully increasing the compound levels already present in the body, serving as another positive point for the therapeutic role of this prostaglandin compound as it thus avoids the need to artificially introduce excess 15d-PGJ_2 into the patient's system. All of the aforementioned, though, is mainly speculative and serves as a promising justification for further analysis and further basic research into this topic.

In this regard, a very important point to address is that more experiments with animal models would be required to obtain data necessary for any type of further research in the direction of 15d-PGJ_2 serving an therapeutic role. However, the current research using *in vivo* xenograft models for 15d-PGJ_2 testing show results that are still very scattered and lacking a unanimous, conclusive answer to the question regarding the effects of 15d-PGJ_2 on tumor growth and especially lacking in demonstrating its effects on the remaining bodily metabolism [84, 100-101].

Therefore, in terms of current research of 15d-PGJ_2, there is still more work needed in elucidating the details of its anti-cancer effects. There still exists a number of potential basic intracellular mechanisms which signify these effects in osteosarcoma that have not yet been fully explained. Interestingly, and offering itself as a good example of data which points to further questions and presents a good example of currently known data that requires a more in-depth analysis is the fact that MG-63, an OS cell line, displayed both a strong anti- and pro-apoptotic response, while the Saos-2 and U2-OS cell lines seem to display only the pro-apoptotic characteristics when treated with the same concentration of 15d-PGJ_2 [91, 92].

Our study confirmed and broadened these results in terms of showing the strong pro-apoptotic effects that 15d-PGJ_2 elicits in the OS cells used. Our results showed previously unreported microscopically observable effects of the lipid compound on the cancer cell morphology, motility as well as the capability of OS cells to multiply and form colonies – a crucial characteristics that tumor cells utilize for growth and spreading.

However, going into more intracellular mechanisms of the 15d-PGJ_2-caused effects on OS cells, we also managed to pinpoint one of the earliest triggers of the reaction cascade leading to these effects. Specifically, this was found to be the triggering of the fast increase of ROS production within the OS cells shortly after the 20 μM 15d-PGJ_2 treatment (as early as one minute post-treatment). This is in alignment with the fact that an increased intracellular ROS formation is a reaction often present in several other analysis of anti-tumor effects on various tumor types, such as colon cancer, breast cancer and leukemia [26-29, 51], but it is also in alignment with the data shown by previous data published on the 15d-PGJ_2-caused ROS increase in OS cells [91-92]. However, due to the incomplete analysis of these phenomena in the U2-OS and Saos-2 cell lines, we decided to test this in more detail. This is of special interest since both of our cell lines of interest are known to be different from MG-63 in their modus operandi, with Saos-2 being a tumorigenically weaker tumor cell line and U2-OS tumorigenically stronger [105]. Another interesting fact gained through our results was that both cell lines showed mutual similarities, at least on the level of post-treatment MAPK protein expression. The sole difference being that the ROS production in each of the two cell lines is achieved by different ROS-scavenger compounds. Namely, PDTC had a stronger ROS attenuation on U2-OS cells while Tempol showed minimal effects, whereas in the case of Saos-2, Tempol showed stronger ROS and subsequent MAPK inhibition while PDTC showed no effect. This should be further analyzed, as the varying reaction to different ROS inhibitors might give us more information on the oxygen species-related changes within the cells after the treatment with 15d-PGJ_2. Our work therefore not only confirmed the presence of a significant and time-dependent increase of 15d-PGJ_2-triggered increase in ROS activity, but it also pinpointed just how early and rapidly this reaction occurs, postulating it as a one of the few very first intracellular effects of the substance within an OS cancer cell (as we've observed both in U2-OS and Saos-2 cell lines).

One of the common downstream targets of a heightened ROS production are the MAPKs. However, the ultimate effect of this signaling event on cell viability can vary. Namely, MAPKs (especially ERK1/2) have been described to trigger both anti- and pro-apoptotic mechanisms, depending on the experimental conditions and on the cell line. MAPKs frequently

trigger anti-apoptotic mechanism via an upregulation of the Bcl-2 pathway [106]. They have also been very often proven to hold strongly pro-apoptotic capabilities. Most commonly this is achieved through their effects on transcription regulators AP-1 and p53, and their power to increase the activity of pro-apoptotic enzymes such as Bax and Bim [107-111]. Interestingly, even their effect on Bcl-2 can be of a dual nature, as it has been proven that p38 and JNK in particular can also have a suppressive effect on the enzyme, therefore triggering a pro-apoptotic effect [112, 113]. Moreover, the connection between a ROS-mediated MAPK activation in particular has also already been proven to present a potent pro-apoptotic mechanism in various cell types, including cancer cells [114-118]. Taken together with our results of the effect of 15d-PGJ_2 on ROS and subsequently MAPK expression, we can conclude that a similarly pro-apoptotic mechanism is extremely highly likely to be occurring in our cells of question as well. This also fits with our observance of the strikingly quick apoptosis activation which is parallel to the ROS activation rise, as well as the rise of MAPK phosphorylation activity.

It is also important to note that ROS play an important role in many anti-tumorigenic mechanisms, often acting as one of the early triggers of cancer cell death, often working in tandem with NADPH (nicotinamide adenine dinucleotide phosphate) to assert its increase and activity [119]. Moreover, ROS increase has been shown to be triggered by 15d-PGJ_2 in the cases of colorectal cancer cells as well as leukemia cells [84]. In the cases of these two cancer cell line, cytosolic NADPH oxidase and mitochondria (complex 1 and 3) appeared to be one of the main sources of ROS generation [82, 119]. This was also confirmed by the usage of EUK-134, a catalase activity mimicking salen-manganese complex antioxidant, which was aimed to block the otherwise present PARP cleavage [84].

A reaction that follows, and seems to be directly triggered by ROS production, is a following rapid increase in intracellular MAPK activation. This is an early cell reaction often present in conditions where a tumor tissue is exposed to an anti-tumorigenic compound. The MAPK that are most often activated in these cases are p38, JNK and ERK1/2, which fits our findings as well [91]. Due to the fact that previous investigations in MG-63 OS cells showed a similar MAPK activation trend, we were curious how an inhibition of the ROS increase might impact the behavior of MAPK activation increase post-treatment in U2-OS and Saos-2 cell lines. By testing the ERK1/2 expression post-ROS scavenger co-treatment, we have demonstrated correlating clear direct correlation between these two, pointing towards a clear importance of the ROS increase within the OS cells in the context of triggering a quick MAPK activation (noted by phosphorylation levels increasing as soon as five minutes post-treatment).

Our results thus strongly confirmed the connection between growing levels of ROS and growing levels of MAPK phosphorylation in the 15d-PGJ_2-triggered signaling cascade. Seeing as the activation of MAPK proteins is often one of the key components in the apoptotic pathway reactions in various cancer cell lines, as previously stated in this thesis, our results confirm and further elaborate how these enzymes, in tandem with ROS, seem to play an equally important role in OS cells as well.

ROS increase is one of the key indicators of increased levels of the intracellular oxidative stress. It can lead to the structural change of redox-sensitive thiols acting as intracellular sensors for the cell redox status. Thioredoxin (Trx) is one example of a protein that is a well-investigated thiol-sensitive redox sensor. Trx uses ways of cysteine thiol-disulfide exchange to reduce various intracellular protein expressions and to actively react to ROS level changes within the cell. Through all of these reactions, ROS plays an important role during the induction of cell death and can be used to monitor this, as well as to monitor the cell oxidation status. To further explain the works of Trx in stress-affected cells, it is important to note that these reactions are initiated by the formation of an inactive complex between Trx1 and the signaling kinase 1 (ASK1). The resulting complex can inhibit the reaction necessary for a full enzymatic activity, namely, the homophilic interaction of the aforementioned ASK1 signaling kinase. Full kinase activity, on the other hand, is achieved through an oxidation of Trx1, which causes a dissociation of Trx1 from the ASK1 protein. ASK1 is also known as a MAP3 kinase, meaning it is capable of directly causing a downstream activation of p38 and JNK, both of which promote the eventual signaling pathway leading to cell apoptosis [120].

15d-PGJ_2 is known to be an electrophile able to modify the Trx thiols through a process known as the Michael adduct formation [121]. Thus, we have decided to test the responsiveness of our osteosarcoma cells to dh-15d-PGJ_2, a 15d-PGJ_2 compound variant lacking a particular electrophilic C9 atom within its chemical structure. The results showed a complete lack of PARP cleavage in the isoform-treated cells, as well as a lack of caspase 3 cleavage. This indicates that the electrophilic C9 carbon atom in 15d-PGJ_2 structure is a key structural feature, necessary for the 15d-PGJ_2-induced apoptotic effects. We speculate that this process is most likely mediated through the de-repression of the ASK1 signalosome and the resulting time-dependent activation of the pro-apoptotic MAP kinases that we can see in our results as well.

Also notable is that the previous work of our group with a different OS cell line (Mg-63) [91] showed that similar intracellular behavior could trigger not only apoptotic effects but also

a significantly strong cell-protective mechanism fueled by several known anti-oxidant-acting proteins. Thus, it was our goal to analyze if this would be the case with Saos-2 and U2-OS cells as well or if these protein expression trends would differ in any way. In our study, we focused on a relevant selection of anti-oxidative response proteins related to this observation which are commonly increased when an intercellular survival mechanism is initiated within a cell under conditions of intracellular stress. Namely these proteins of interest were Nrf2, Akt NF-κB, and Egr1. [102-104] Unlike what was observed in similar 15d-PGJ_2 experiments in MG-63 cells, the expression of all of the aforementioned proteins showed solely a consistent and steady decline. Nrf2 as well as the NF-κB expression decrease, along with the markedly increased cell apoptosis, fits to the results obtained by 15d-PGJ_2 treatment of cisplatin-resistant Saos-2 and MG-63 cells and the 15d-PGJ_2 treatment of breast cancer cells [89, 92]. Fitting with our results are also previous experiments with 15d-PGJ_2 and its effect on OS cells within the context of 15d-PGJ_2 effect on anti-oxidant-related proteins such as Akt, Nrf2 and NF-kB. Similar Akt decrease was measured, albeit at a later time point, in U2-OS cells [92]. This also correlated with increased apoptosis. Altogether, our results indicate a strong confirmation of 15d-PGJ_2 being unable to activate any significantly strong cytoprotective mechanism in U2-OS and Saos-2 cells, unlike what was previously observed in MG-63 cells [91]. A potential explanation for this may be the previously noted difference in tumorigenicity as well as clonogenicity levels, as well as genetic background differences of those three OS cell lines.

In relation to this, we have to point out that a lack of focus on the genetic differences of various OS cell lines presents an example of a weak point of this work so far, as it has not been investigated in detail yet. p53 and Rb are the main genes known to be responsible for triggering the osteosarcoma development and growth. Within tumor cells, they are responsible for regulatory mechanisms affecting DNA damage response, cell cycle arrest responses, as well as cell death triggering [1-4]. In the three mentioned osteosarcoma cell lines, both of these genes are expressed differently. Namely, MG-63 is known to express a functional Rb gene while it is negative for p53. U2-OS cells, on the other hand, express both Rb and p53 genes, while Saos-2 cells lacks a positive expression of both [122-123].

These characteristics should be the focus of future work, where it would be indicative to attempt suppression of either Rb, p53 or both of the two tumor suppressor genes and to observe the way the protein expression cascade unfolds under these conditions. As these genes and proteins are dysfunctional in a variety of tumor tissues, a valid hypothesis might be

that changing or subduing their expression status might significantly impact the toxic effect a compound (such as 15-PGJ2 in this case) may have on the osteosarcoma cells. In our case, even though the three cell lines vary in expression of p53 and RB, the one major difference noticeable was in comparison with the previous work done in regards to the effect of 15d-PGJ_2. Namely, 15d-PGJ_2, as previously stated, caused a successful co-activation of an anti-oxidant pathway along with an apoptotic one. In the cause of U2-OS and Saos-2, this wasn't the case as the apoptotic pathway overpowered any potential cytoprotective mechanism very early into the treatment (within two hours of 15d-PGJ_2 treatment). However, the genetic variability between the cell lines could cause possibly be present on a more detailed level or it may lie in different so far untested branches of the intracellular signaling pathways. Therefore, this focus point should be explored further.

Next, we attempted to bridge the challenging gap between *in vitro* and *in vivo* that is often present in OS research. We did this by using a *semi-in vivo* method – the CAM assay. Using a simple grafting method, CAM assay can be used to administer and grow a wide variety of cells on a live chicken chorioallantoic membrane, allowing the cells to grow, thrive, and form a tissue. Another advantage of this experimental model is that it does not require an approval of the ethical committee. Therefore, CAM assay presents itself as a fairly quick, efficient and practical system to test cell and tissue reactions to various substances, to test cell drug-intake, as well as to observe the beginning stages of biological cell phenomena such as cancer cell angiogenesis [94].

OS in particular is one of the cell subtypes that has been shown to grow successfully on the CAM and, therefore, allows this method to be used in early stages of potential drug investigation on this type of cells. One study confirming this used 8 OS cell line panel. It aimed to show the capability of each cell line to survive and form tumors on the CAM. Within the mentioned study, Saos-2 and U2-OS cells showed prominent cell growth and survival whereas MG-63 demonstrated only moderate tumor growth on the CAM [124]. In our study, we have noticed a somewhat different result, namely, we have observed that all three OS cell lines (Saos-2, U2-OS, and MG-63) displayed a capability of forming solid tumors on the CAM. However, the aforementioned 8 panel experimental work had used and *in ovo* CAM method, while we employed the *ex ovo* CAM method. Such a difference in growth conditions is subtle, but may cause a slight difference in the integrity and sensitivity of the CAM tissue as well as of the embryo status beneath the CAM.

Conclusively, we have described the way 15d-PGJ_2 activates the apoptotic pathway within U2-OS and Saos-2 cell lines. What differs our study from study published so far is also that we focused mainly on the early aspects and triggers of these events, as well as on the determination of precise time points for particular cell events. The fast and efficient reaction that the 15d-PGJ_2 causes within the OS cells strongly indicated 15d-PGJ_2 as a potential therapeutic agent. This is further emphasized by two important facts: i) 15d-PGJ_2 is naturally occurring, ii) the effects in parallel viability experiments show a significantly lesser negative impact on the non-malignant osteoblast cells (which serve as origin cells and surrounding cell tissue of most OS cell lines). Altogether, our results represent a strong basis for further investigations of this substance as an anti-OS therapeutic agent.

Based on our results, the general findings regarding the protein cascade and molecular mechanism involved in the conclusions are presented in the schematic below. This schematic is also presented as an ultimate conclusion of our research paper whose results are the basis of this thesis, and which is cited at the beginning of this thesis.

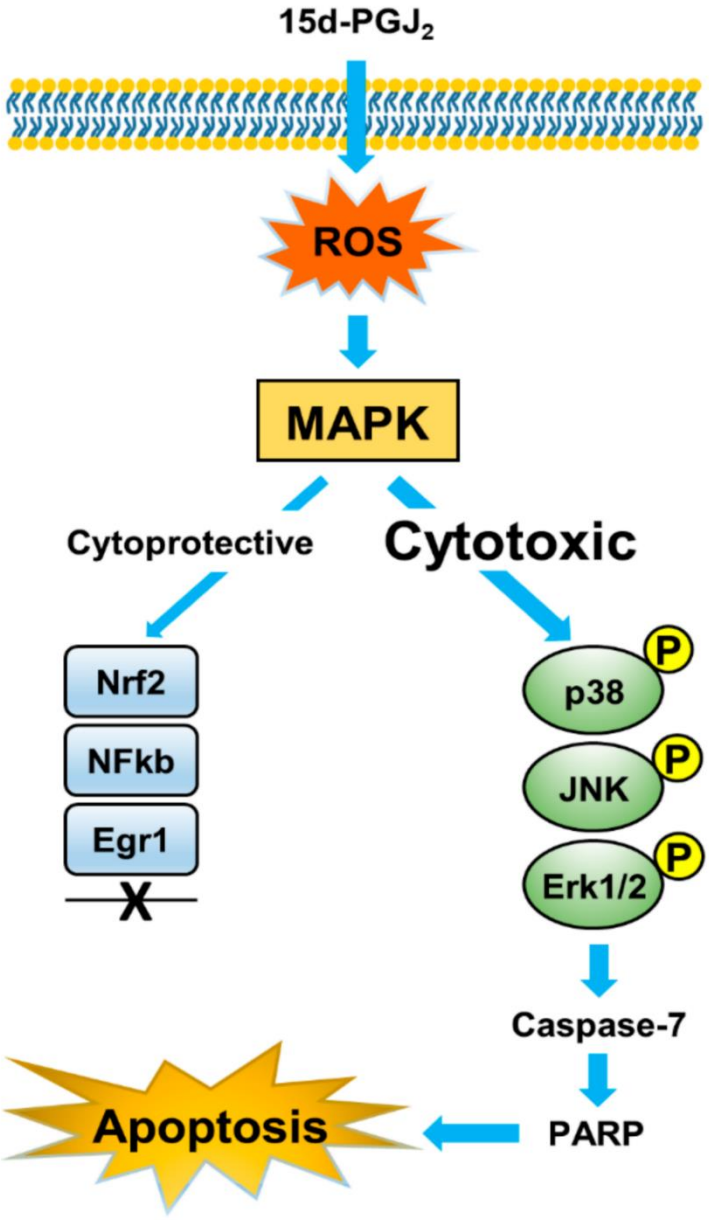

Image 2. ***15d-PGJ$_2$-induced apoptotic pathway schematic*** *(reproduced from [96] with permission of MDPI publisher, Basel, Switzerland)*

Conclusively, the strong connection between 15d-PGJ_2 and the strong oxidative response it triggers, further setting in motion the rest of the signaling cascade towards apoptosis, is a mechanism that should be explored further. Seeing as the ROS response has been so powerful, exploring the effect of the prostaglandin compound on intracellular iNOS levels could provide the next step in this direction of research. iNOS has been shown to act in a particularly dual manner in terms of cancer regulation and it still remains a puzzling component of many anti-tumor responses worthy of being further investigated in terms of its involvement in many anti-tumor-acting compounds [124-125].

Finally, to provide further detail into our attempt to elucidate the earliest characteristics of the effects 15d-PGJ_2 has on OS cells, another target in need of tackling via additional extensive research is the exploration of any and all receptors involved in the reaction between this prostaglandin compound and the OS cells. As previously stated, the PPAR family of receptors is the one often involved in the relationship between 15d-PGJ_2, however, in the context of OS, this has not yet been proven and is where the following focus should be aimed towards, with additional attention to other potential receptors involved, seeing as the compound-receptor-cell communication is an absolutely vital component of refining a fully understood and well researched compound with an anti-therapeutic future.

In summary, our work has provided an solid and favorable outlook on the cytotoxic qualities that 15d-PGJ_2 holds when administered as a treatment on OS cells, a conclusion which we have enriched when compared to the previous work done in relation to this topic, as well as expanded with further details outlining its intracellular effects. On one hand, our findings have cleared a number of questions focused on the intracellular events occurring at the earliest activation stages of the 15d-PGJ_2-induced signaling pathway within our OS cell lines. On the other hand, we have also broadened the current knowledge of how the apoptotic effects of this substance impact certain tumorigenic properties of the OS cancer cells such as colony formation capability as well as general cell mobility. The connection between these effects and a profound intracellular oxidative response is one of the additional strong and crucial links in these events and our additional elucidations of the currently known data on this matter also help in opening up several possibilities of further explorations of this particular phenomena and how it aids the 15d-PGJ_2-induced cell toxicity. Conclusively, the successful application of the CAM assay also further confirmed our conclusions regarding the properties of the compound against OS by acting as a viable semi-*in* vivo method and providing an

additional level of high potential assuredness and optimism in regards to the possibility and encouragement of 15d-PGJ_2 being further researched and assessed in the direction of it potentially serving as an apt therapeutic agent, or therapeutic aid, against OS.

5. BIBLIOGRAPHY

1. Lindsey BA, Markel JE, Kleinerman ES. Osteosarcoma Overview. Rheumatol Ther. 2017;4(1):25–43.
2. Misaghi A, Goldin A, Awad M, Kulidjian AA. Osteosarcoma: a comprehensive review. SICOT-J. 2018/04/09. 2018;4:12.
3. Broadhead ML, Clark JCM, Myers DE, Dass CR, Choong PFM. The Molecular Pathogenesis of Osteosarcoma: A Review. Kovar H, editor. Sarcoma. 2011;2011:959248.
4. Mei J, Zhu X-Z, Wang Z-Y, Cai X-S. Functional outcomes and quality of life in patients with osteosarcoma treated with amputation versus limb-salvage surgery: a systematic review and meta-analysis. Arch Orthop Trauma Surg. 2014 Sep;134.
5. Hayden JB, Hoang BH. Osteosarcoma: basic science and clinical implications. Orthop Clin North Am. 2006 Jan;37(1):1–7.
6. Meazza C, Scanagatta P. Metastatic osteosarcoma: a challenging multidisciplinary treatment. Expert Rev Anticancer Ther. 2016 May;16(5):543–56.
7. Stiller CA, Bielack SS, Jundt G, Steliarova-Foucher E. Bone tumours in European children and adolescents, 1978-1997. Report from the Automated Childhood Cancer Information System project. Eur J Cancer. 2006 Sep;42(13):2124–35.
8. Cotterill SJ, Wright CM, Pearce MS, Craft AW. Stature of young people with malignant bone tumors. Pediatr Blood Cancer. 2004 Jan;42(1):59–63.
9. Sisu AM. On the Bone Tumours: Overview, Classification, Incidence, Histopathological Issues, Behavior and Review Using Literature Data. In: Stana LG, editor. Rijeka: IntechOpen; 2012. p. Ch. 4.
10. Marko TA, Diessner BJ, Spector LG. Prevalence of Metastasis at Diagnosis of Osteosarcoma: An International Comparison. Pediatr Blood Cancer. 2016 Jun;63(6):1006–11.
11. Marina N, Gebhardt M, Teot L, Gorlick R. Biology and therapeutic advances for pediatric osteosarcoma. Oncologist. 2004;9(4):422–41.
12. Bacci G, Longhi A, Versari M, Mercuri M, Briccoli A, Picci P. Prognostic factors for osteosarcoma of the extremity treated with neoadjuvant chemotherapy: 15-year experience in 789 patients treated at a single institution. Cancer. 2006 Mar;106(5):1154–61.

13. Lagmay JP, Krailo MD, Dang H, Kim A, Hawkins DS, Beaty O 3rd, et al. Outcome of Patients With Recurrent Osteosarcoma Enrolled in Seven Phase II Trials Through Children's Cancer Group, Pediatric Oncology Group, and Children's Oncology Group: Learning From the Past to Move Forward. J Clin Oncol Off J Am Soc Clin Oncol. 2016 Sep;34(25):3031–8.

14. Anninga JK, Gelderblom H, Fiocco M, Kroep JR, Taminiau AHM, Hogendoorn PCW, et al. Chemotherapeutic adjuvant treatment for osteosarcoma: where do we stand? Eur J Cancer. 2011 Nov;47(16):2431–45.

15. Howlader N, Noone AM, Krapcho M, Neyman N, Aminou R, Waldron W, Altekruse SF, Kosary CL, Ruhl J, Tatalovich Z, Cho H, Mariotto A, Eisner MP, Lewis DR, Chen HS, Feuer EJ, Cronin KA (eds). SEER Cancer Statistics Review, 1975-2009 (Vintage 2009 Populations), National Cancer Institute. Bethesda, MD, https://seer.cancer.gov/archive/csr/1975_2009_pops09/, based on November 2011 SEER data submission, posted to the SEER web site, April 2012.

16. Rickel K, Fang F, Tao J. Molecular genetics of osteosarcoma. Bone. 2017 Sep;102:69–79.

17. Wu C-C, Livingston JA. Genomics and the Immune Landscape of Osteosarcoma. Adv Exp Med Biol. 2020;1258:21–36.

18. Kovac M, Blattmann C, Ribi S, Smida J, Mueller NS, Engert F, et al. Exome sequencing of osteosarcoma reveals mutation signatures reminiscent of BRCA deficiency. Nat Commun . 2015;6(1):8940.

19. Shimatani A, Aono M, Hoshi M, Oebisu N, Iwai T, Takada N, et al. Secondary osteosarcoma in patients previously treated for childhood cancer: Three case reports. Mol Clin Oncol. 2019 Jan;10(1):153–8.

20. Sofka CM, Ciavarra G, Saboeiro G, Ghelman B. Paget's disease of the spine and secondary osteosarcoma. HSS J . 2006 Sep;2(2):188–90.

21. WHO Classification of Tumours Editorial Board. Soft Tissue and Bone Tumours (WHO Classification of Tumours). 5th Edition, Volume 3. France: World Health Organisation; 2020.

22. Mito JK, Mitra D, Barysauskas CM, Mariño-Enriquez A, Morgan EA, Fletcher CDM, et al. A Comparison of Outcomes and Prognostic Features for Radiation-Associated Angiosarcoma of the Breast and Other Radiation-Associated Sarcomas. Int J Radiat Oncol Biol Phys. 2019 Jun;104(2):425–35.

23. Ottaviani G, Jaffe N. The epidemiology of osteosarcoma. Cancer Treat Res. 2009;152:3–13.

24. Meister P, Konrad EA, Stotz S. Extraskeletal Osteosarcoma. Case report and differential diagnosis. Arch Orthop Trauma surgery Arch fur orthopadische und Unfall-Chirurgie. 1981;98(4):311–4.
25. Kunze B, Bürkle S, Kluba T. Multifocal osteosarcoma in childhood. Chir Organi Mov. 2009 May;93(1):27–31.
26. Hermann G, Klein MJ, Springfield D, Abdelwahab IF, Dan SJ. Intracortical osteosarcoma; two-year delay in diagnosis. Skeletal Radiol. 2002 Oct;31(10):592–6.
27. Ferguson JL, Turner SP. Bone Cancer: Diagnosis and Treatment Principles. Am Fam Physician. 2018 Aug;98(4):205–13.
28. Pant S, Tripathi S, Dandriyal R, Astekar M, Joshi A. Osteosarcoma: A Diagnostic Dilemma. J Exp Ther Oncol. 2017 May;12(1):61–5.
29. Wittig JC, Bickels J, Priebat D, Jelinek J, Kellar-Graney K, Shmookler B, et al. Osteosarcoma: a multidisciplinary approach to diagnosis and treatment. Am Fam Physician. 2002 Mar;65(6):1123–32.
30. Whelan JS, Jinks RC, McTiernan A, Sydes MR, Hook JM, Trani L, et al. Survival from high-grade localised extremity osteosarcoma: combined results and prognostic factors from three European Osteosarcoma Intergroup randomised controlled trials. Ann Oncol Off J Eur Soc Med Oncol. 2011/10/19. 2012 Jun;23(6):1607–16.
31. Gröbner SN, Worst BC, Weischenfeldt J, Buchhalter I, Kleinheinz K, Rudneva VA, et al. The landscape of genomic alterations across childhood cancers. Nature. 2018;555(7696):321–7.
32. McMahon KR, Harel-Sterling M, Pizzi M, Huynh L, Hessey E, Zappitelli M. Long-term renal follow-up of children treated with cisplatin, carboplatin, or ifosfamide: a pilot study. Pediatr Nephrol. 2018 Dec;33(12):2311–20.
33. Robison LL, Hudson MM. Survivors of childhood and adolescent cancer: life-long risks and responsibilities. Vol. 14, Nature reviews. Cancer. 2014. 61–70.
34. Simbre VC, Duffy SA, Dadlani GH, Miller TL, Lipshultz SE. Cardiotoxicity of cancer chemotherapy: implications for children. Paediatr Drugs. 2005;7(3):187–202.
35. Iyer NS, Balsamo LM, Bracken MB, Kadan-Lottick NS. Chemotherapy-only treatment effects on long-term neurocognitive functioning in childhood ALL survivors: a review and meta-analysis. Blood. 2015 Jul;126(3):346–53.
36. Picci P, Mercuri M, Ferrari S, Alberghini M, Briccoli A, Ferrari C, et al. Survival in high-grade osteosarcoma: improvement over 21 years at a single institution. Ann Oncol Off J Eur Soc Med Oncol. 2010 Jun;21(6):1366–73.

37. Janeway KA, Barkauskas DA, Krailo MD, Meyers PA, Schwartz CL, Ebb DH, et al. Outcome for adolescent and young adult patients with osteosarcoma: a report from the Children's Oncology Group. Cancer. 2012 Sep;118(18):4597–605.
38. Wippel B, Gundle KR, Dang T, Paxton J, Bubalo J, Stork L, et al. Safety and efficacy of high-dose methotrexate for osteosarcoma in adolescents compared with young adults. Cancer Med. 2018/12/22. 2019 Jan;8(1):111–6.
39. Aggerholm-Pedersen N, Rossen P, Rose H, Safwat A. Pazopanib in the Treatment of Bone Sarcomas: Clinical Experience. Transl Oncol . 2019/12/23. 2020 Feb;13(2):295–9.
40. Belayneh R, Fourman MS, Bhogal S, Weiss KR. Update on Osteosarcoma. Curr Oncol Rep. 2021;23(6):71.
41. Beck O, Paret C, Russo A, Burhenne J, Fresnais M, Steimel K, et al. Safety and Activity of the Combination of Ceritinib and Dasatinib in Osteosarcoma. Cancers (Basel). 2020 Mar;12(4):793.
42. Ricciotti E, FitzGerald GA. Prostaglandins and inflammation. Arterioscler Thromb Vasc Biol. 2011 May;31(5):986–1000.
43. Scher JU, Pillinger MH. The anti-inflammatory effects of prostaglandins. J Investig Med Off Publ Am Fed Clin Res. 2009 Aug;57(6):703–8.
44. Wang D, Dubois RN. Prostaglandins and cancer. Gut. 2006 Jan;55(1):115–22.
45. Kobayashi K, Omori K, Murata T. Role of prostaglandins in tumor microenvironment. Cancer Metastasis Rev. 2018 Sep;37(2–3):347–54.
46. Ladas EJ, Jacobson JS, Kennedy DD, Teel K, Fleischauer A, Kelly KM. Antioxidants and cancer therapy: a systematic review. J Clin Oncol Off J Am Soc Clin Oncol. 2004 Feb;22(3):517–28.
47. Jara-Gutiérrez Á, Baladrón V. The Role of Prostaglandins in Different Types of Cancer. Cells. 2021 Jun;10(6).
48. Gamradt SC, Feeley BT, Liu NQ, Roostaeian J, Lin YQ, Zhu LX, et al. The effect of cyclooxygenase-2 (COX-2) inhibition on human prostate cancer induced osteoblastic and osteolytic lesions in bone. Anticancer Res. 2005;25(1A):107–15.
49. Zhang X, Schwarz EM, Young DA, Puzas JE, Rosier RN, O'Keefe RJ. Cyclooxygenase-2 regulates mesenchymal cell differentiation into the osteoblast lineage and is critically involved in bone repair. J Clin Invest. 2002 Jun;109(11):1405–15.
50. Pilbeam C. Prostaglandins and Bone. Handb Exp Pharmacol. 2020;262:157–75.

51. Raisz LG. Prostaglandins and bone: physiology and pathophysiology. Osteoarthr Cartil. 1999 Jul;7(4):419–21.
52. Sakuma S, Usa K, Fujimoto Y. The regulation of formation of prostaglandins and arachidonoyl-CoA from arachidonic acid in rabbit kidney medulla microsomes by linoleic acid hydroperoxide. Prostaglandins Other Lipid Mediat. 2006 May;79(3–4):271–7.
53. Eschwège P, de Ledinghen V, Camilli T, Kulkarni S, Dalbagni G, Droupy S, et al. [Arachidonic acid and prostaglandins, inflammation and oncology]. Presse Med. 2001 Mar;30(10):508–10.
54. Korbecki J, Baranowska-Bosiacka I, Gutowska I, Chlubek D. The effect of reactive oxygen species on the synthesis of prostanoids from arachidonic acid. J Physiol Pharmacol an Off J Polish Physiol Soc. 2013 Aug;64(4):409–21.
55. Jang Y, Kim M, Hwang SW. Molecular mechanisms underlying the actions of arachidonic acid-derived prostaglandins on peripheral nociception. J Neuroinflammation. 2020 Jan;17(1):30.
56. Attiq A, Jalil J, Husain K, Ahmad W. Raging the War Against Inflammation With Natural Products. Front Pharmacol. 2018;9.
57. Yue L, Durand M, Lebeau Jacob MC, Hogan P, McManus S, Roux S, et al. Prostaglandin D2 induces apoptosis of human osteoclasts by activating the CRTH2 receptor and the intrinsic apoptosis pathway. Bone. 2012 Sep;51(3):338–46.
58. Figueiredo-Pereira ME, Corwin C, Babich J. Prostaglandin J2: a potential target for halting inflammation-induced neurodegeneration. Ann N Y Acad Sci. 2016 Jan;1363(1):125–37.
59. Li J, Guo C, Wu J. 15-Deoxy-Δ-(12,14)-Prostaglandin J2 (15d-PGJ2), an Endogenous Ligand of PPAR-γ: Function and Mechanism. PPAR Res. 2019 Aug;2019:7242030.
60. Das S, Chandrasekhar S, Yadav JS, Grée R. Recent Developments in the Synthesis of Prostaglandins and Analogues. Chem Rev . 2007 Jul 1;107(7):3286–337.
61. Zhang X, Schwarz EM, Young DA, Puzas JE, Rosier RN, O'Keefe RJ. Cyclooxygenase-2 regulates mesenchymal cell differentiation into the osteoblast lineage and is critically involved in bone repair. J Clin Invest. 2002 Jun;109(11):1405–15.

62. Obermajer N, Wong JL, Edwards RP, Odunsi K, Moysich K, Kalinski P. PGE(2)-driven induction and maintenance of cancer-associated myeloid-derived suppressor cells. Immunol Invest. 2012;41(6–7):635–57.
63. Pettipher R. The roles of the prostaglandin D(2) receptors DP(1) and CRTH2 in promoting allergic responses. Br J Pharmacol. 2007/10/29. 2008 Mar;153 Suppl 1(Suppl 1):S191–9.
64. Morteau O. Prostaglandins and inflammation: the cyclooxygenase controversy. Arch Immunol Ther Exp (Warsz). 2000;48(6):473–80.
65. Uchida K, Shibata T. 15-Deoxy-Delta(12,14)-prostaglandin J2: an electrophilic trigger of cellular responses. Chem Res Toxicol. 2008 Jan;21(1):138–44.
66. Morgenstern J, Fleming T, Kadiyska I, Brings S, Groener JB, Nawroth P, et al. Sensitive mass spectrometric assay for determination of 15-deoxy-Δ(12,14)-prostaglandin J(2) and its appcation in human plasma samples of patients with diabetes. Anal Bioanal Chem. 2017/11/16. 2018 Jan;410(2):521–8.
67. Bie Q, Dong H, Jin C, Zhang H, Zhang B. 15d-PGJ2 is a new hope for controlling tumor growth. Am J Transl Res. 2018 Mar;10(3):648–58.
68. Álvarez-Almazán S, Bello M, Tamay-Cach F, Martínez-Archundia M, Alemán-González-Duhart D, Correa-Basurto J, et al. Study of new interactions of glitazone's stereoisomers and the endogenous ligand 15d-PGJ2 on six different PPAR gamma proteins. Biochem Pharmacol. 2017 Oct;142:168–93.
69. Kroker AJ, Bruning JB. Review of the Structural and Dynamic Mechanisms of PPARγ Partial Agonism. PPAR Res. 2015;2015:816856.
70. Richard AJ, Stephens JM. The role of JAK-STAT signaling in adipose tissue function. Biochim Biophys Acta . 2013/06/02. 2014 Mar;1842(3):431–9.
71. Degrelle SA, Shoaito H, Fournier T. New Transcriptional Reporters to Quantify and Monitor PPARγ Activity. PPAR Res. 2017;2017:6139107.
72. Ricote M, Li AC, Willson TM, Kelly CJ, Glass CK. The peroxisome proliferator-activated receptor-gamma is a negative regulator of macrophage activation. Nature. 1998 Jan;391(6662):79–82.
73. Marcone S, Evans P, Fitzgerald DJ. 15-Deoxy-Δ(12,14)-Prostaglandin J(2) Modifies Components of the Proteasome and Inhibits Inflammatory Responses in Human Endothelial Cells. Front Immunol. 2016;7:459.
74. Meng Y, Chen C, Tian C, Du J, Li H-H. Angiotensin II-Induced Egr-1 Expression is Suppressed by Peroxisome Proliferator- Activated Receptor-γ Ligand 15d-PGJ2 in Macrophages. Cell Physiol Biochem. 2015;35(2):689–98.

75. Maehara T, Nakamura T, Maeda S, Aritake K, Nakamura M, Murata T. Epithelial cell-derived prostaglandin D(2) inhibits chronic allergic lung inflammation in mice. FASEB J Off Publ Fed Am Soc Exp Biol. 2019 Jul;33(7):8202–10.

76. Coutinho DS, Anjos-Valotta EA, do Nascimento CVMF, Pires ALA, Napimoga MH, Carvalho VF, et al. 15-Deoxy-Delta-12,14-Prostaglandin J(2) Inhibits Lung Inflammation and Remodeling in Distinct Murine Models of Asthma. Front Immunol. 2017;8:740.

77. Huang L, Li G, Feng X, Wang L. 15d-PGJ2 Reduced Microglia Activation and Alleviated Neurological Deficit of Ischemic Reperfusion in Diabetic Rat Model. Biomed Res Int. 2015;2015:864509.

78. Xu F, Li J, Ni W, Shen Y, Zhang X. Peroxisome proliferator-activated receptor-γ agonist 15d-prostaglandin J2 mediates neuronal autophagy after cerebral ischemia-reperfusion injury. PLoS One. 2013;8(1):e55080.

79. Mateu A, Ramudo L, Manso MA, De Dios I. Cross-talk between TLR4 and PPARγ pathways in the arachidonic acid-induced inflammatory response in pancreatic acini. Int J Biochem Cell Biol. 2015 Dec;69:132–41.

80. Bianchi A, Moulin D, Hupont S, Koufany M, Netter P, Reboul P, et al. Oxidative stress-induced expression of HSP70 contributes to the inhibitory effect of 15d-PGJ2 on inducible prostaglandin pathway in chondrocytes. Free Radic Biol Med. 2014;76:114–26.

81. Chen S, Liu C, Wang X, Li X, Chen Y, Tang N. 15-Deoxy-Δ12,14-prostaglandin J2 (15d-PGJ2) promotes apoptosis of HBx-positive liver cells. Chem Biol Interact. 2014;214:26–32.

82. Moloney JN, Cotter TG. ROS signalling in the biology of cancer. Semin Cell Dev Biol. 2018 Aug;80:50–64.

83. Arfin S, Jha NK, Jha SK, Kesari KK, Ruokolainen J, Roychoudhury S, et al. Oxidative Stress in Cancer Cell Metabolism. Antioxidants (Basel, Switzerland). 2021 Apr 22;10(5):642.

84. Shin S-W, Seo C-Y, Han H, Han J-Y, Jeong J-S, Kwak J-Y, et al. 15d-PGJ2; Induces Apoptosis by Reactive Oxygen Species–mediated Inactivation of Akt in Leukemia and Colorectal Cancer Cells and Shows Antitumor Activity. Clin Cancer Res. 2009 Sep;15(17):5414 LP – 5425.

85. Chen S-Y, Lu F-J, Gau R-J, Yang M-L, Huang T-S. 15-Deoxy-delta12,14-prostaglandin J2 induces apoptosis of a thyroid papillary cancer cell line (CG3 cells)

through increasing intracellular iron and oxidative stress. Anticancer Drugs. 2002 Aug;13(7):759–65.

86. Toaldo C, Pizzimenti S, Cerbone A, Pettazzoni P, Menegatti E, Daniela B, et al. PPARgamma ligands inhibit telomerase activity and hTERT expression through modulation of the Myc/Mad/Max network in colon cancer cells. J Cell Mol Med. 2010 Jun;14(6A):1347–57.

87. Kulkarni AA, Woeller CF, Thatcher TH, Ramon S, Phipps RP, Sime PJ. Emerging PPARγ-Independent Role of PPARγ Ligands in Lung Diseases. PPAR Res. 2012;2012:705352.

88. Fujita M, Tohji C, Honda Y, Yamamoto Y, Nakamura T, Yagami T, et al. Cytotoxicity of 15-deoxy-Δ(12,14)-prostaglandin J(2) through PPARγ-independent pathway and the involvement of the JNK and Akt pathway in renal cell carcinoma. Int J Med Sci. 2012;9(7):555–66.

89. Muhammad SNH, Mokhtar NF, Yaacob NS. 15d-PGJ2 Induces Apoptosis of MCF-7 and MDA-MB-231 Cells via Increased Intracellular Calcium and Activation of Caspases, Independent of ERα and ERβ. Asian Pac J Cancer Prev. 2016;17(7):3223-9.

90. Han H, Shin S-W, Seo C-Y, Kwon H-C, Han J-Y, Kim I-H, et al. 15-Deoxy-delta 12,14-prostaglandin J2 (15d-PGJ2) sensitizes human leukemic HL-60 cells to tumor necrosis factor-related apoptosis-inducing ligand (TRAIL)-induced apoptosis through Akt downregulation. Apoptosis. 2007 Nov;12(11):2101–14.

91. Koyani CN, Kitz K, Rossmann C, Bernhart E, Huber E, Trummer C, et al. Activation of the MAPK/Akt/Nrf2-Egr1/HO-1-GCLc axis protects MG-63 osteosarcoma cells against 15d-PGJ2-mediated cell death. Biochem Pharmacol. 2016 Mar;104:29–41.

92. Yen C-C, Hsiao C-D, Chen W-M, Wen Y-S, Lin Y-C, Chang T-W, et al. Cytotoxic effects of 15d-PGJ2 against osteosarcoma through ROS-mediated AKT and cell cycle inhibition. Oncotarget; 2014: 5 (3).

93. Kawahito Y, Kondo M, Tsubouchi Y, Hashiramoto A, Bishop-Bailey D, Inoue K, et al. 15-deoxy-delta(12,14)-PGJ(2) induces synoviocyte apoptosis and suppresses adjuvant-induced arthritis in rats. J Clin Invest. 2000 Jul;106(2):189–97.

94. Deryugina EI, Quigley JP. Chick embryo chorioallantoic membrane model systems to study and visualize human tumor cell metastasis. Histochem Cell Biol. 2008/11/13. 2008 Dec;130(6):1119–30.

95. Doyle K, Fitzpatrick FA. Redox signaling, alkylation (carbonylation) of conserved cysteines inactivates class I histone deacetylases 1, 2, and 3 and antagonizes their transcriptional repressor function. J Biol Chem. 2010/04/12. 2010 Jun 4;285(23):17417–24.

96. Mikulčić M, Tabrizi-Wizsy NG, Bernhart EM, Asslaber M, Trummer C, Windischhofer W, et al. 15d-PGJ2 Promotes ROS-Dependent Activation of MAPK-Induced Early Apoptosis in Osteosarcoma Cell In Vitro and in an Ex Ovo CAM Assay. Int J Mol Sci. 2021 Oct;22(21).

97. Higuchi T, Miyake K, Oshiro H, Sugisawa N, Yamamoto N, Hayashi K, et al. Trabectedin and irinotecan combination regresses a cisplatinum-resistant osteosarcoma in a patient-derived orthotopic xenograft nude-mouse model. Biochem Biophys Res Commun. 2019 May:513(2):326–31.

98. Grignani G, D'Ambrosio L, Pignochino Y, Palmerini E, Zucchetti M, Boccone P, et al. Trabectedin and olaparib in patients with advanced and non-resectable bone and soft-tissue sarcomas (TOMAS): an open-label, phase 1b study from the Italian Sarcoma Group. Lancet Oncol. 2018 Oct;19(10):1360–71.

99. Powell WS. 15-deoxy-Δ12,14-PGJ2: endogenous PPARγ ligand or minor eicosanoid degradation product? J Clin Invest. 2003 Sep 15;112(6):828–30.

100. Trindade-da-Silva CA, Reis CF, Vecchi L, Napimoga MH, Sperandio M, Matias Colombo BF, et al. 15-Deoxy-Δ(12,14)-prostaglandin J2 Induces Apoptosis and Upregulates SOCS3 in Human Thyroid Cancer Cells. PPAR Res. 2016;2016:4106297.

101. Collantes M, Martínez-Vélez N, Zalacain M, Marrodán L, Ecay M, García-Velloso MJ, et al. Assessment of metabolic patterns and new antitumoral treatment in osteosarcoma xenograft models by [18F]FDG and sodium [18F]fluoride PET. BMC Cancer. 2018;18(1):1193.

102. Koundouros N, Poulogiannis G. Phosphoinositide 3-Kinase/Akt Signaling and Redox Metabolism in Cancer. Front Oncol. 2018;8.

103. Pagel J-I, Deindl E. Disease progression mediated by egr-1 associated signaling in response to oxidative stress. Int J Mol Sci. 2012 Oct;13(10):13104–17.

104. Wardyn JD, Ponsford AH, Sanderson CM. Dissecting molecular cross-talk between Nrf2 and NF-κB response pathways. Biochem Soc Trans. 2015/08/03. 2015 Aug;43(4):621–6.

105. Lauvrak SU, Munthe E, Kresse SH, Stratford EW, Namløs HM, Meza-Zepeda LA, et al. Functional characterisation of osteosarcoma cell lines and identification of

mRNAs and miRNAs associated with aggressive cancer phenotypes. Br J Cancer. 2013/09/24. 2013 Oct;109(8):2228–36.

106. Lu Z, Xu S. ERK1/2 MAP kinases in cell survival and apoptosis. IUBMB Life. 2006 Nov;58(11):621–31.

107. Yue J, López JM. Understanding MAPK Signaling Pathways in Apoptosis. Int J Mol Sci. 2020 Mar;21(7).

108. Dhanasekaran DN, Reddy EP. JNK signaling in apoptosis. Oncogene. 2008 Oct;27(48):6245–51.

109. Cuenda A, Rousseau S. p38 MAP-kinases pathway regulation, function and role in human diseases. Biochim Biophys Acta. 2007 Aug;1773(8):1358–75.

110. Zeke A, Misheva M, Reményi A, Bogoyevitch MA. JNK Signaling: Regulation and Functions Based on Complex Protein-Protein Partnerships. Microbiol Mol Biol Rev. 2016 Sep;80(3):793–835.

111. Kim BJ, Ryu SW, Song BJ. JNK- and p38 kinase-mediated phosphorylation of Bax leads to its activation and mitochondrial translocation and to apoptosis of human hepatoma HepG2 cells. J Biol Chem. 2006 Jul;281(30):21256–65.

112. Farley N, Pedraza-Alva G, Serrano-Gomez D, Nagaleekar V, Aronshtam A, Krahl T, et al. p38 mitogen-activated protein kinase mediates the Fas-induced mitochondrial death pathway in CD8+ T cells. Mol Cell Biol. 2006 Mar;26(6):2118–29.

113. Inoshita S, Takeda K, Hatai T, Terada Y, Sano M, Hata J, et al. Phosphorylation and inactivation of myeloid cell leukemia 1 by JNK in response to oxidative stress. J Biol Chem. 2002 Nov;277(46):43730–4.

114. Wada T, Stepniak E, Hui L, Leibbrandt A, Katada T, Nishina H, et al. Antagonistic control of cell fates by JNK and p38-MAPK signaling. Cell Death Differ. 2008 Jan;15(1):89–93.

115. Hui L, Bakiri L, Mairhorfer A, Schweifer N, Haslinger C, Kenner L, et al. p38alpha suppresses normal and cancer cell proliferation by antagonizing the JNK-c-Jun pathway. Nat Genet. 2007 Jun;39(6):741–9.

116. Zhang X, Wang X, Wu T, Li B, Liu T, Wang R, et al. Isoliensinine induces apoptosis in triple-negative human breast cancer cells through ROS generation and p38 MAPK/JNK activation. Sci Rep. 2015 Jul;5:12579.

117. Bragado P, Armesilla A, Silva A, Porras A. Apoptosis by cisplatin requires p53 mediated p38alpha MAPK activation through ROS generation. Apoptosis. 2007 Sep;12(9):1733–42.

118. Trempolec N, Muñoz JP, Slobodnyuk K, Marin S, Cascante M, Zorzano A, et al. Induction of oxidative metabolism by the p38α/MK2 pathway. Sci Rep. 2017 Sep;7(1):11367.

119. Magnani F, Mattevi A. Structure and mechanisms of ROS generation by NADPH oxidases. Curr Opin Struct Biol. 2019 Dec;59:91–7.

120. Tobiume K, Matsuzawa A, Takahashi T, Nishitoh H, Morita K, Takeda K, et al. ASK1 is required for sustained activations of JNK/p38 MAP kinases and apoptosis. EMBO Rep. 2001 Mar;2 (3):222–8.

121. Shibata T. 15-Deoxy-$\Delta^{12,14}$-prostaglandin J_2 as an electrophilic mediator. Biosci Biotechnol Biochem. 2015: 79(7):1044–9.

122. Montanaro L, Mazzini G, Barbieri S, Vici M, Nardi-Pantoli A, Govoni M, et al. Different effects of ribosome biogenesis inhibition on cell proliferation in retinoblastoma protein- and p53-deficient and proficient human osteosarcoma cell lines. Cell Prolif. 2007 Aug;40(4):532–49.

123. Park Y-B, Park MJ, Kimura K, Shimizu K, Lee SH, Yokota J. Alterations in the INK4a/ARF locus and their effects on the growth of human osteosarcoma cell lines. Cancer Genet Cytogenet. 2002 Mar;133(2):105–11.

124. Kunz P, Schenker A, Sähr H, Lehner B, Fellenberg J. Optimization of the chicken chorioallantoic membrane assay as reliable in vivo model for the analysis of osteosarcoma. PLoS One. 2019 Apr 15;14(4):e0215312–e0215312.

125. Vannini F, Kashfi K, Nath N. The dual role of iNOS in cancer. Redox Biology. 2015: 6: 334-343.

126. Burke A, Sullivan F, Giles F, Glynn S. The yin and yang of nitric oxide in cancer progression. Carcinogenesis. 2013 Mar;34 (3): 503–512.